Reviewer #1 Comments and Response:

This manuscript introduces the measurements of the blowing snow with the Particle Tracking Velocimetry (PTV) and tries to investigate the particle motions near the snow surface. I appreciate very much for the author's effort to apply the PTV technique in the field and successful observations. The attitude should be highly evaluated.

Thank you.

However, as far as I read through the manuscript, I have got the impression that the data shown here is not always valuable for both the drifting and blowing snow research community, in particular, for the accurate modeling.

PTV recordings shown in Figure 2 probably involve the meaningful information, however, I am afraid the surface bed is far from flat and the height difference amounted to 5 mm. It gives the substantial effect on both particle speeds and the wind velocities shown in Figure 3.

Yes, we note the effect of surface "microtopography" on obtaining useable statistics is shown below the dashed line of influence. In the revised paper, we have introduced terrain-following coordinates (see response to Reviewer Comments #2). However, 5 mm rise over 130 mm equates to a little more than 2 degrees of slope. When we are considering blowing snow in alpine terrain, this is quite flat.

(Page 6, 2nd paragraph.)

It is quite plausible that the reason why the wind speed showed the maximum at 2 to 7 mm

We do not see this in our data.

and why a zero wind velocity zone above the saltation layer exists is related to the bed surface undulation.

A modeled zero wind velocity zone above in figure 3e-f could indeed be related to surface roughness. The issue at hand in the discussion is how in natural conditions, the commonly used log-law will predict erroneous wind profiles. Thus the choice of timescales for mean values and assumptions required for predicting wind speed for blowing snow in complex terrain must be of higher concern.

(Section 3.1)

Bagnold's focal point is hard to refer under such conditions. Further, the friction velocity of 0.08 m/s at Rec. #2 is extremely low; under such conditions the blowing snow, never breaks out and keeps going, even though we take into account the turbulence effect.

The wind data for Rec #2 has been compromised during the recording specific period, hence why the

difference between 2m and 40cm values is so much larger than during other recordings. This has been highlighted in the revised text.

(Page 9, line 17).

On the contrary, at Rec. #3, u* is extremely high. Under such conditions, I suppose the particle concentration near the surface increases largely and it makes hard to distinguish individual particle, that is, no precise particle tracking is available.

True, particle tracking does become difficult and this was mentioned in the discussion of figure 4 – (old P10 L24, P11 L4.)

(Page 8, line 23, Page 13, line 8.)

In fact, I cannot agree with you more that the turbulences including ejection and sweep intermittent structures are key factors to initiate the snow particle motion, rather than the time averaged friction velocities, not only in the mountain area but on the flat snow surface.

However, when you would like to set your focus on these issues, you need more specific and detailed analysis based on the high frequency data. Although the quadrant analysis has been tried, the explanation of the outcome is superficial, more detailed analysis related to the particle motion are essential.

Thank you. We have expanded this analysis as well as the amount of data investigated in the revised paper.

(Section 3.1 and Section 3.3)

Presumably 1m distance between the PTV and the anemometer makes the quantitative comparison difficult?

This distance has a considerably smaller effect in the atmospheric surface layer than in wind tunnels because the eddies driving the turbulent structures are much larger. This lateral distance was chosen to preclude any bluff-body influence of the camera/laser apparatus. Subsequent data has been included with a smaller distance between PTV and anemometer in a spanwise orientation. Please refer to the response to Reviewer #2 Comments.

(Page 5, 1st paragraph)

Further, the descriptions in the discussion and conclusion parts are mostly qualitative and look nothing but a pile of well-known and predictable issues.

We have obtained many similar results to aeolian transport studies in much more controlled wind

tunnel environments, this shows how the PTV approach in natural conditions can confirm certain results found in more controlled, but less natural wind tunnel environments. The scientific blowing snow community would benefit from the knowledge that such techniques may be used in nature, as the potential gains from employing these techniques outdoors are considerable, albeit with further quantitative results coming only after "well-known and predictable issues" are first addressed.

More firm conclusions based on the more quantitative analysis are essential. I strongly recommend, first of all, the authors to reexamine the obtained data again and uncover the hiding useful ones.

Data from two more nights of recording have been included in the analysis and discussion in the revised paper. Consideration of these data and further analysis of other data has led to stronger conclusions.

Further, an accumulation of more data will be preferable; in actual, saltation of 400 to 1000μm diameter graupel is a very exceptional case. I cannot believe that such large particles kept saltation under the friction velocity of 0.08 m/s at Rec. #2r.

Addressed above. Improved particle diameter algorithms have been used with particle size distributions included in the Document Supplement Figure 1, as well as mean and max values in Table 1.

Reviewer #2 Comments and Response:

In this paper, the authors describe a set of innovative data acquired by Particle trecking Velocimetry during blowing snow events. Even if Particle Trecking Velocimetry is a classic wind-tunnel method for studying drifting particles, this is the first investigation to measure outdoor snow particle flux and velocity. It is really challenging and interesting and is a potential source of new knowledge. Such experiments should be made known to the scientific community. But even if the paper is potentially interesting, it seems that it is not suited for publication in its current state. I have several suggestions for improvement if the authors would like to resubmit the manuscript.

- (1) The results are not described in sufficient details and conclusions are often not supported through the material presented. The authors must be aware of what information the data can provide and what they cannot provide. It is a persistent problem throughout the whole text. Sometimes, the new findings highlighted in the paper seem questionable.

We have expanded the discussion of results, added new data to back this discussion and included new results that are strongly backed by analysis of this data. We have clarified the findings from the data and removed speculative discussion or identified it more clearly in the discussion section. We are very confident in the veracity and certainty of our results and note that as these come from outdoor measurements, they are more likely to be representative of natural blowing snow than are wind tunnel simulations under less turbulent and more idealized two phase flow conditions.

P7-L10 : From figures 3a-g, it is not evident that the constant particle velocity gradient is limited to a height below 10 mm, at least for me.

After consideration, we agree with this comment and so have expanded our analysis with new data and now Figure 3 has been restructured using terrain following coordinates. Now, particle velocity profiles of 12 recordings (9 new) over three nights of recordings are presented encompassing 283 seconds and 513,000 frames. From these we have found that the horizontal velocity profiles of ascending particles start to diverge from linear plots above heights that vary from 8 to 15 mm.

Moreover it seems that the velocity gradient estimated by linear regression includes all measurements points? Is it the case?

In the new figure 3, the velocity gradient has been estimated using particles in the first 10 mm of the terrain following coordinate system.

How do the authors estimate that this 10 mm transition corresponds with the upper extent of the low-energy population?

As noted above we no longer conclude that there is a 10 mm threshold (pg. 12 l. 5-10,). Aeolian transport exhibits a continuous spectrum of particle velocities and so the gradient of motions

from "low-energy" to "high-energy" does not contain a discrete step. Using the Ho et al. (2014) definition, derived for saltating sand in a wind tunnel, where the two populations are distinguishable if grains are either responsive or irresponsive to changes in 'wind strength,' we found that nearly all snow particles outdoors are responsive to 'wind strength'. This manuscript has been restructured to discuss this continuum of motion through examination of particle velocity distributions (as in Ho et al. 2012) and identifying the region of transition from a creep dominated particle population to higher energy grains. This highlights the important role of creep in forming the lower boundary condition and "source" for saltation.

P8-L14: The 10 mm threshold delimitating variances of blowing snow particles is not clear again. The decline in variances is not so pronounced. For sure it is difficult to directly estimate this value from the graph. Some orders of magnitude could be useful for the readers.

We agree. The variance argument has been eliminated and replaced by data in a new Figure 3.

P9-L4 : I did not understand how the results help to illuminate the shift in snow transport mechanics when transitioning to particles in the tail of particles velocity distributions. The authors are expected to provide more explicit demonstration.

This is now explicitly demonstrated as follows: This and other studies have shown that the density of flow decreases exponentially with height. The two particle velocity histograms (above and below 4mm) indicated at what velocities the majority of particles were moving in each height region. 4 mm was an arbitrary divide to separate near surface and above surface flow regions. Very close to the surface in the densest part of the flow, the flux was dominated by slow moving ("creep") particles, but also with a contribution of relatively fewer high-energy ("saltation") particles that has not been described before. Above the snow surface, there was a continuum of particle velocities that was dominated by high-energy particles. The increasing proportion of high-energy particles with distance from the surface is due to the need for a greater velocity to reach greater heights on a ballistic trajectory from the surface and the subjection to stronger winds with increasing distance above the surface.

We were illuminating the point that high energy particles are also counted at the <4mm level as well. Therefore typical saltation measurements that limit data above the creep layer are missing critical data, whereas, near-surface measurements include both populations. Additionally, there is an intrinsic coupling of low-energy ("creep") population with high-energy ("saltation") particles as they both occupy the same spatial location, and the creep layer feeds upper regions of saltation as mentioned in the new discussion of Figure 4 (Figure 9).
(Pg 15-16.)

P10 : The authors have to explain in details how concurrent streamwise wind measurements show penetration of a turbulent sweep.

Figure 4 has now been adapted (Figure 8) to show time periods of significant ejection and

sweep using Quadrant Analysis with a hole size of 1. There is an ejection (triangles) that precedes the main sweep (dots) event at 8 seconds. Sweeps by definition indicate positive fluctuations in streamwise wind speed with negative fluctuations in the vertical. As the sweep first became evident at 2 m and then at 0.4 m height, this motion clearly penetrated from above.

The discussion in the manuscript discusses these issues at length now,
(Section 3.3, pg 17 line 19, pg 18 line 19.)

Why is it best to base our reasoning on streamwise wind measurements instead of Reynolds stress measurements?

This is an excellent question. This empirical finding from our data agrees with conclusions from other field and wind tunnel sand studies (Bauer et al., 1998; Sterk et al., 1998; Schonfeldt and von Lowis 2003, Leenders 2005). Strong ejections (high Reynolds stress) events at 2-4 second, and >12 seconds did not result in blowing snow transport. Instead it was the positive fluctuations in streamwise wind speed that resulted in flux. The nature of turbulence near the surface has an influence of transport initiation and a simple Reynolds stress cannot fully describe this, whilst near surface wind speeds can better reflect sweeps and ejection events. Further analysis of this phenomenon is of interest but would be a very extensive addition to this paper and so we now call for it in the conclusions and suggest it for future research.
(Pg 11 line 3, pg 23)

P10-L4 (and figure 4): New threshold values (4 mm and 8 mm) are given in this paragraph. Without any additional measurements, I see absolutely no reason why the authors change their tune. The authors previously compared the 10 mm threshold with values obtained by Ho et al., 2014, which correspond to the limit between saltation and reptation (particles are divided in two populations on the basis whether or not they rise high enough to be affected by the flow strength).

These three arbitrary heights are <u>not thresholds</u>, they were chosen to illuminate the subtle differences in particle transport and the continuum of motion as grains begin motion and begin bouncing to greater heights as wind speeds increase. They do not indicate hard thresholds of "creep" versus "saltation" regimes.

This will be reflected more clearly in the text to avoid such misinterpretations. In the revised text we have adopted the Ho et al. (2012) probability distribution explanation of "long tails" corresponding to the population of high energy grains.
(Pg 4, line 2, 5, 9-10. Pg 15, line 12 to Pg 16 line 5. Pg 17, line 26, pg 20, line 26, Page 21 line 6)

On which basis (other than a qualitative approach for one blowing snow event) do the authors decide that 4 mm is the limit between creep and saltation? It is really confusing.

This arbitrary height is <u>not a threshold</u>, it was chosen to illuminate the subtle differences in particle transport and the continuum of motion as grains begin motion and begin bouncing to greater heights as wind speeds increase. To clarify, we have revised the text to more clearly show a transition

region between the "creep" dominated and "full saltation" dominated flow regions. This was already mentioned several times in the text. The emphasis is that the creep layer contributes substantially to blowing snow flux and is the source of saltation.
(Pg 4, line 2, 5, 9-10. Pg 15, line 12 to Pg 16 line 5. Pg 17, line 26, pg 20, line 26, Page 21 line 6 Pg 12, line 11.)

P9-L16 : How do the authors consider that particles are in creep? by the position of the particles (i.e a particle seen below 4 mm is considered as being in creep ?) If at a given time a particle is at this position, it doesn't mean that later it will not be able to rise high enough to be affected by the flow strength.

As explained above, we do not use a height threshold, but examine particle speed and consider a continuum of motions between classical creep and saltation. The histogram in figure 3 (now Figure 7) was designed for this purpose: low-energy particles near the surface are more likely to be "creep". (page 9 second paragraph). The difference line on P9 – L16 identifies precisely the low-energy particles present near the surface, whereas the high-energy particles that are present at both heights are not counted. This is emphasized clearly in the revised paper.
(Pg 16, line 7.)

(2) It is surprising that the results are not discussed taking into consideration key measurement uncertainties (related to the position of surface bed and to the distance between PTV measurements and ultrasonic anemometer). This way, analysis could be enhanced.

Natural blowing snow as found outdoors has a naturally uneven bed – in contrast to its common representation in wind tunnel studies. Uncertainty with respect to the position of the bed is briefly addressed with respect to the line indicating "influence of microtopography" in figure (2, 3). The issue of surface influence is now considered quantitatively by using a terrain-following coordinate system.
(Page 6 2nd paragraph)

Measurement uncertainties with respect to the distance between PTV and ultrasonic wind measurements can be considered negligible for time-averaged quantities as they are occurring at similar heights. Assuming Taylor's frozen turbulence hypothesis, and utilizing the mean wind speed during recordings, a lag time of approximately 1/3 of a second could be expected, much shorter than the duration of any given recording. For instantaneous measurement comparisons, these lag times are discussed in that section.

The February 3 and March 3 laser measurements were made at closer distances (0.5 and 0.33 m, respectively) to the CSATs, perpendicular to the direction of wind flow. The effect of this orientation on comparing turbulence to transport measurements is mentioned in the revised text.
(Page 5, 1st paragraph . Page 23, line 11.)

- (3) The time series need to be extended, as –apparently- there are much more data available. However, it would be useful to know how many other cases (if any) could have been selected and

why they were not presented here. I would encourage the authors to present more of the valuable data. If not, the research paper must be considered as a Brief communication (http://www.the-cryosphere.net/about/manuscript_types.html)

We only wanted to include data for which we had the highest confidence. Other videos from the 2014-2015 field campaign were not presented because there were either not sufficient particles in transport to give meaningful average profiles, or the particle flows were too dense and obscured illumination. We have now added new data from the 2016 field campaign – there is now more than six times the length of the original data available for analysis and has allowed more certain generalization of the results to inform the conclusions.
(Page 7, line 6-25. Page 8 line 10-15.)

-relating to the item 3

Neutral stability did not occur during the field campaign as it can be seen on table 1 (the Reynolds stress is not constant with the height). It is a pity because neutral con- ditions are quite usual on the site (80% of the 192 hourly periods studied in Helgason and Pomeroy, 2005).

The Helgason and Pomeroy (2005) Kananaskis valley bottom site is 14 km away and 600 m lower than this high alpine valley site and so stability is not really comparable between them. This distinction is made clearer in the revised paper. But it was very useful that you pointed this out. Correcting a numerical error now shows, using both Monin-Obuhkov and the bulk/gradient Richardson number approaches, that there are indeed near-neutral (slightly stable) conditions on the nights of Mar 23, Feb 3 and Mar 3. All three nights are now part of the analysis and discussion and are further detailed in the revisions.
(Page 9, line 1. Supplementary Document, Figure 1-3)

So, authors can't calculate the aerodynamic roughness which becomes a function of height.

Exactly, this is one complication we wished to highlight for use of log-law models that drive blowing snow in complex terrain. The discrepancy in roughness length measurements is evident in Table 1. There are somewhat more consistent values of z_0 on Feb 3 and Mar 3 for some of the recordings, now included in the new Table 1 (Table 2).
(Page 9, line 20 to Page 11 line 7.)

What are the Richardson numbers for these experiments? Is there any other data under neutral stability over the course of the campaign?

Plots of the Richardson numbers for the near-neutral conditions on Mar 23, Feb 3, and Mar 3 are supplied as well as the Min, and Max values during the periods of active blowing snow recording (highlighted blocks in the time series). Slightly stable conditions occurred on all nights, and this correction is included in the revised paper. Monin-Obukhov length also indicates slightly stable

conditions during all recording periods.
(Supplementary Document, Figure 1-3)

For recording 2 there is a strong difference between u* estimated by eddy covariance method at a height of 200 cm and a height of 40 cm. Is it possible for the blowing particles to disturb the measurements?

Yes, it appears that was the case. While the noise did not greatly affect the mean wind speed (there is reasonable agreement between 40 cm and 200 cm averages), there was sufficient noise in the signal to obscure the turbulence measurements. This is noted in the revised paper.
(Page 9 line 17).

What are the drifting snow fluxes measured during recording-only period and during the 15 minutes surrounding each recording.

Equivalent diameters of individual blowing snow particles were measured in each frame, allowing a spherical estimate of the blowing snow volume in the 2mm wide plane of illumination. This is similar to the sand and snow studies of Creysells et al. (2009), Guo et al. (2013), and Paterna et al. (2016) among others. The time series of volume fraction was then multiplied by the density of ice by the average particle velocity for each time step to obtain a mass flux of blowing snow Q_s in $kg\ m^{-2}s^{-1}$. Averaging these values over the duration of a recording gives a mean blowing snow flux rate for given wind and snow conditions. Values of Q_s are now included in the wind characteristics Table 2.
(Page 8 line 4-9)

There are quite unusual results which need to be commented (for example high value of roughness which can be smaller when estimating by flux-profile estimation techniques suggesting that the mean wind profile was in equilibrium with the snow surface, however the turbulence was not (Helgason and Pomeroy, 2005).

We do not attempt to estimate roughness from the wind speed profile given the violation of fully developed log-linear law assumptions. This is quite different from H and P's situation where time-averaged log-linear profiles appeared to be valid. However the high roughness lengths due to high turbulence appear to be characteristics of both sites due to their mountain location. This is commented on further in the revised paper.
(Section 3.1)

- (4) The text could be more concise and focused. Similar points are discussed in several places of the text.
-relating to the item 4

P7-L10/20 : Paragraph about Ascending particles
P7-L21/P8-L8 : Paragraph about Descending particles
P8-L9/P8-L14: Paragraph about Ascending particles. It is a little bit confusing for the reader-

Thank you for this excellent suggestion. These sections have been reorganized.

- (5) Moreover the nature of discussion should be more quantitative than qualitative.
relating to the item 5

Figure 5 by itself is not an evidence that tumblons eroded many smaller crystals from the surface or shattered themselves and immediately became saltating grains, depending on impact velocity. Where are the measurements to show the effect of impact velocity? Moreover impacting particles may travel transverse to the plane of light and may not be included on the second image. Conclusions must be based on a statistical approach.

Tumblons have not been identified before in two-phase flow and their initial description here is necessarily mainly qualitative. The point of their inclusion in the paper is to distinguish the types of motion found in natural, outdoor blowing snow from that found in sand or found in wind tunnels. Figure 5 has been removed and the reference has been changed to supplemental videos, with overlain PTV vector fields, of tumblons that both shatter upon impact and tumble along the surface with. To better quantify them, we now compare the impact velocity of the shattering tumblon and that which remained whole.
Shattering Tumblon: $< u, v > \approx < 2.46, -.43 >$ ms^{-1}
Rolling tumblon: $< u, v > \approx < 0.6, .1 > ms^{-1}$ *(depending on what is considered center of mass).*

- (6) Papers supporting the reasoning should be properly referenced and used. Otherwise, it puts a doubt into readers' minds.
-relating to the item 6
P3- L7: Ho et al., 2011 does not address grain velocity distribution functions

Thank you - corrected.

P8-L27: Ho et al., 2012 deals with Particle velocity distribution in saltation transport. So when speaking about number density, the authors have to use the right reference (It is probably Ho et al., 2011).

Thank you - corrected.

Ho et al., 2011 explained that the particle volume fraction decreases with height at a given exponential rate in saltation layer. If the authors want to compare their results with Ho et al., 2011, they have to limit the analysis to the first centimeter and to draw the result in the same manner as Ho et al., 2011 (figure 8) with an inset including the characteristic decay length.

This has been done for 12 videos over the nights of Mar 23 2015, and Feb 3 and Mar 3 2016. Because our study is concerned with highly intermittent conditions, we profiled average particle

number flux (number of particles in transport multiplied by average particle velocity at that height). With 100% tracking, in equilibrium wind tunnel conditions, this value is theoretically equal at every time step. As our time series include periods of developing and no flux, a temporal average of particle fraction would not be comparable to the results of Ho et al. (2011). Instead, we limit our attention to only periods when transport was occurring. Notably, this means the characteristic decay lengths are not "apples to apples" comparable with Ho et al. 2011, but the fraction of total flux at each height in our profiles is representative of a plot that could be generated by Ho et al. (2011) data. Analysis of changes between our decay lengths in the style of Ho et al. (2011) is possible for our data set has been conducted.

This is discussed in more detail in the revised paper.
(Figure 7, Page 14, line 3-21. Page 21, last paragraph)

Moreover the authors base their analysis on the fractional particle number flux whereas Ho et al., 2011 base their analysis on the particle volume fraction. If both results are compared, the authors have to take into account the volume of particles which can vary according to the wind speed.

The methods of obtaining the two data sets, and the values under comparison are now more clearly distinguished. The difference between mass flux (or volume fraction) and number flux has been mentioned in the text with respect to the ability of the tracking algorithm to capture the flux: "As noted elsewhere (Creyssels et al., 2009), particle-tracking algorithms in the densest regions of saltation are still problematic, and thus these are conservative underestimates of near-surface flux." –page 9.

This is discussed in more detail in the revised paper:
(Page 14, last paragraph, Page 15, line 3-9, Page 21 last paragraph)

P2-L29: Schmidt (1980) instead of Schmidt (1986)

Thank you - corrected.

P11-L18/24: Sugiura and Maeno, 2000 made a distinction between horizontal restitution coefficient and vertical coefficient restitution, which are different from the restitution coefficient calculated from the authors. Moreover the calculation method completely differs. The authors should make it clear.

We have now noted that we used a different method, and that because of the density of flow a statistical method was necessary: A particle by particle restitution was not possible because the tracking software used often re-identified a rebounded particle as distinct from an incoming particle. Therefore a bulk statistical approach was used, what was the average incoming versus the average outgoing velocity. Looking in a region >1 particle diameter above the surface, we hoped to measure a rebound coefficient for truly rebounding particles, and not including reptating grains, which would artificially lower the coefficient. In the revised paper, we have lifted the region to 6 mm ($\pm$ 2 mm) in terrain following coordinates above the surface.

Additionally, because we are dealing with a natural surface topography, not a smooth bed as found in wind tunnel studies, parsing out horizontal and vertical restitution coefficients is not beneficial as the impact angle depends largely on the location of impact. A more general approach of E_xy does not require distinguishing the location of impact and provides information on kinetic redistribution and grain-bed impact elasticity useful for momentum balance concerns.
(Page 16, First Paragaph)

P7-L19: What is the numerical value of the transition height obtained by Ho et al., 2014 (2zf) ? As far I can see from Figure 3 the Bagnold focus point zf is around 8 mm. Considering uncertainties in relation to the choice of 10 mm threshold both values are close together.

The Bagnold focus point is unavailable for us to identify, as the wind profile did not remotely follow a log-linear scale as would be found for a prairie sites (Pomeroy and Gray, 1990). This is expected given the non-steady state conditions. Therefore, a log-linear profile with a linear offset (addition of U_f term) does not fit either. Attempts to fit it with and without the Bagnold focal point produced focal point values ranging from 11 mm to nearly 6 m!
(Page 10, line 5)

What are the Shield numbers of the snow particles in the experiments? Ho et al., 2014 remain that the results have been obtained in a finite range of Shields number from 0.04 to 0.2.

Shields numbers ranged from 0.006 to 0.2. This is now indicated in the wind characteristics table 2.
(Page 12, line 23, Page 13, line 2.)

Bauer, B. ., J. Yi, S. Namikas, and D. Sherman (1998), Event detection and conditional averaging in unsteady aeolian systems, *J. Arid Environ.*, *39*, 345–375.

Creyssels, M., P. Dupont, a. O. El Moctar, A. Valance, I. Cantat, J. T. Jenkins, J. M. Pasini, and K. R. Rasmussen (2009), Saltating particles in a turbulent boundary layer: experiment and theory, *J. Fluid Mech.*, *625*, 47–74, doi:10.1017/S0022112008005491.

Guo, L., and N. Huang (2013), Wind tunnel studies on the vertical emission of sand grains from surface, in *AIP Proceedings 1542*, vol. 1087, pp. 1087–1089.

Helgason, W., and J. Pomeroy (2005), Uncertainties in estimating turbulent fluxes to melting snow in a mountain clearing, in *Proc. 62nd Eastern Snow Conf*, pp. 129–142.

Ho, T. D., A. Valance, P. Dupont, and A. Ould El Moctar (2011), Scaling laws in aeolian sand transport, *Phys. Rev. Lett.*, *106*(9), 4–7, doi:10.1103/PhysRevLett.106.094501

Ho, T. D., P. Dupont, A. Ould El Moctar, and A. Valance (2012), Particle velocity distribution in saltation transport, *Phys. Rev. E - Stat. Nonlinear, Soft Matter Phys.*, *85*(5), 1–5, doi:10.1103/PhysRevE.85.052301.

Ho, T. D., A. Valance, P. Dupont, and A. Ould El Moctar (2014), Aeolian sand transport: Length and height distributions of saltation trajectories, *Aeolian Res.*, *12*, 65–74, doi:10.1016/j.aeolia.2013.11.004.

Paterna, E., P. Crivelli, and M. Lehning (2016), Decoupling of mass flux and turbulent wind fluctuations in drifting snow, *Geophys. Res. Lett.*, 1–7, doi:10.1002/2016GL068171.

Pomeroy, J., and D. Gray (1990), Saltation of snow, *Water Resour. Res.*, *26*(7), 1583–1594.

Schönfeldt, H.-J., and S. von Löwis (2003), Turbulence-driven saltation in the atmospheric surface layer, *Meteorol. Zeitschrift*, *12*(5), 257–268, doi:10.1127/0941-2948/2003/0012-0257.

Sterk, G., a. F. G. Jacobs, and J. H. Van Boxel (1998), The effect of turbulent flow structures on saltation sand transport in the atmospheric boundary layer, *Earth Surf. Process. Landforms*, *23*(10), 877–887, doi:10.1002/(SICI)1096-9837(199810)23:10<877::AID-ESP905>3.0.CO;2-R.

Near-Surface Snow Particle Dynamics from Particle Tracking Velocimetry and Turbulence Measurements during Alpine Blowing Snow Storms

Nikolas O. Aksamit[1], John W. Pomeroy

[1]Centre for Hydrology, University of Saskatchewan, Saskatoon, S7N 5C8, Canada

Correspondence to: Nikolas O. Aksamit (n.aksamit@usask.ca)

Abstract. Many blowing snow conceptual and predictive models have been based on simplified two-phase flow dynamics derived from time-averaged observations of bulk flow conditions in blowing snow storms. Measurements from the first outdoor application of Particle Tracking Velocimetry (PTV) of near-surface blowing snow yields new information on mechanisms for blowing snow initiation, entrainment, and rebound, whilst also confirming some findings from wind tunnel observations. Blowing snow particle movement is influenced by complex surface flow dynamics, including saltation development from creep that has not previously been measured for snow. Comparisons with 3D atmospheric turbulence measurements show that blowing snow particle motion immediately above the snow surface responds strongly to high frequency turbulent motions. Momentum exchange from wind to the dense near-surface particle-laden flow appears significant and makes an important contribution to blowing snow mass flux and saltation initiation dynamics. The more complete and accurate description of near-surface snow particle motions observable using PTV may prove useful for improving blowing snow model realism and accuracy.

1 Introduction

Wind transport of snow influences the variability of alpine summer runoff (*Pomeroy et al.*, 2012; *Winstral et al.,* 2013), is a large contributor to the growth or ablation of small mountain glaciers (*Dyunin and Kotlyakov*, 1980), and can contribute snow loading to avalanche prone areas (*Schweizer et al*., 2003). Time-averaged blowing snow field measurements often present an oversimplified view of a highly variable and unsteady natural phenomenon. Physical snow trap mechanisms only provide mass

flux averages over prolonged collection periods (*Budd et al.*, 1966). Snow particle counters only recently began providing point measurements of particle speed (*Nishimura et al.,* 2014) along with particle size and number flux values (*Schmidt*, 1984; *Brown and Pomeroy*, 1989; *Kinar and Pomeroy,* 2015). Snow traps and particle counters can neither measure the mechanisms of transport initiation nor provide continuous vertical profiles of particle concentration or transport. Yet, most current blowing snow model development has been informed from time-averaged measurements from such devices. Accordingly, simplified models of blowing snow persist in the literature that do not contain self-consistent wind-snow momentum balances, as demonstrated by *Andreotti* (2004) for sand. As well, there is a current lack of detailed measurements of particle-surface interactions in natural conditions.

Nik Aksamit 8/31/2016 2:41 PM
Deleted: simple

Nik Aksamit 8/31/2016 2:41 PM
Deleted:).

Nik Aksamit 8/31/2016 2:41 PM
Deleted: as a

Recent progress in blowing snow research has been accelerated by novel applications of high-speed imaging systems. *Kobayashi* (1972) pioneered blowing snow recordings with outdoor, 1/8-second shutter speed images. This was the first visual evidence of particle mechanics in the snow saltation layer and was extremely informative in the development of saltation theory (*Pomeroy and Gray*, 1995), but the photographs consisted of blurred snow particle streaks or were saturated with particles, disguising individual particle motions. More recently, *Gordon and Taylor* (2009) designed a novel and effective halogen backlit camera system to effectively obtain particle size and shape parameters in the Arctic, but were limited to an imaging area on the order of 9 mm^2. In a further study, *Gordon et al.* (2009) modified this technique to image an area of 124 mm x 101 mm with a black and white binarization algorithm to obtain continuous particle density profiles. Unfortunately, particle velocity measurements were unavailable from either study.

In laboratories, several wind tunnel studies have examined drifting snow with Particle Image Velocimetry (PIV) (*Lu et al.,* 2012; *Tominaga et al.*, 2012), shadowgraphy (*Gromke et al*., 2014) and shadowgraphic Particle Tracking Velocimetry (PTV) (*Groot Zwaaftink et al.*, 2014; *Paterna et al.*, 2016), providing valuable insights into saltating snow velocity distributions, average relative wind and saltating snow velocities, particle size distributions, qualitative comparisons to Large Eddy Simulation driven transport, and equilibrium wind-blowing snow decoupling. Blowing snow transport model development continues to address small-scale variability (e.g. *Nemoto and Nishimura*, 2004; *Groot Zwaaftink et al*., 2014), and requires advanced measurement techniques to understand the physics

Nik Aksamit 8/31/2016 2:41 PM
Deleted: and

driving such multi-scale heterogeneities as well as evaluate the uncertainties and assumptions inherent in proposed models.

Of the multitude of blowing snow models that have been developed, many implement components of earlier aeolian saltation or initiation models, e.g. the work of *Bagnold* (1941), *Owen* (1964), *Schmidt* (1980), *Pomeroy and Gray* (1990), and *Nishimura and Hunt* (2000). In what follows, effort has been made to refer only to the original work containing the model component or measurement campaign under discussion, but comments generally apply to all derivatives. Following the work of *Bagnold* (1941), current theory often represents blowing snow in two layers, saltation and suspension, with a neglected and poorly understood creep mechanism at the lower boundary of saltation (*Pomeroy and Gray*, 1990; *Nishimura and Hunt*, 2000; *Doorschot and Lehning*, 2002). Once the wind surpasses a transport threshold velocity, saltating particles follow ballistic trajectories, and rebound off the surface, rising no higher than 10 cm. As wind speeds increase, saltating particles become suspended by turbulence and disperse upwards. Closely following wind streamlines, suspended particles rarely encounter the ground (*Pomeroy and Male*, 1992; *Bintanja*, 2000).

The two most commonly modeled modes of saltation initiation are *aerodynamic lift*, the direct drag induced ejections of grains, and *splash*, the ejection of grains by rebounding saltating particles (*Doorschot and Lehning*, 2002, *McElwaine et al.,* 2004). However, there are substantial disagreements about these mechanisms; *Schmidt* (1986) calculated that direct aerodynamic lift was not possible under average flow conditions over a level snow surface due to strong snow particle bonding. *Doorschot et al.* (2004) argued the fragile dendritic snow in their study resulted in aerodynamic lift dominance. It is likely that both mechanisms are possible and that the prevalent mechanism depends on the wind conditions and snow surface structure and cohesion. There is a growing pool of blowing snow models parameterizing these two initiation mechanisms, including the work of *Doorschot and Lehning* (2002), *Nemoto and Nishimura* (2004) and *Groot Zwaaftink et al.* (2014), all adapting the blowing sand initiation model of *Anderson and Haff* (1991) through wind tunnel measurements.

In contrast to representing saltation as a layer of particles moving with uniform trajectories (e.g. *Owen*, 1964) as is common in snow saltation studies (*Pomeroy and Gray*, 1990; *Tabler*, 1991; *Doorschot and Lehning*, 2002), recent wind tunnel studies and numerical simulations of wind transport of sand have

Nik Aksamit 8/31/2016 2:41 PM
Deleted: *Pomeroy* (1988) was unable to identify different threshold wind speeds for either aerodynamic lift or particle splash to dominate.

Nik Aksamit 8/31/2016 2:41 PM
Deleted: i.

Nik Aksamit 8/31/2016 2:41 PM
Formatted: Font:Italic

shown the benefit of representing saltation with continuous grain velocity distribution functions (*Creysells et al.,* 2009; *Ho et al.,* 2012, 2014). From these observations, two populations of saltating particles are distinguishable by kinetic energy rather than by physical properties such as grain size. High-energy particles have higher and longer trajectories that are influenced by changes in wind strength. However, these particles only constitute the long tails of velocity distribution functions (*Ho et al.,* 2012). The bulk of sand saltation observed in these studies consists of low-energy splashed 'ejecta' and tractating (bed transport) grains undergoing very short hops. These grains generate the majority of mass flux and govern the mean properties of equilibrium saltation (*Ho et al*., 2014).

As saltation develops, transport mechanics evolve. For instance, in sand, saltation and creep transport modes are often coupled when saltation begins (*Willets et al.,* 1991): as low-energy surface particles accelerate, they begin feeding upper regions of saltation. Allowing variability of motion in blowing snow saltation models permits consideration of additional mechanisms of saltation initiation and momentum transfer to the snow surface.

It remains unknown how well recent advances in conceptualization of blowing sand transport can improve descriptions of blowing snow because detailed observations of outdoor blowing snow particle transport processes near the snow surface have not been conducted. Perhaps due to this, current theories of snow saltation are inconsistent with each other and conceptualize a limited range of snow motions and initiation mechanisms. To improve the physical theory of blowing snow initiation and transport, this study demonstrates PTV as a tool for measuring short timescale blowing snow surface motions in an outdoor environment. The objectives of this study are to examine the mechanics of snow particle motion initiation, the detailed interactions between wind speed fluctuations and snow particle dynamics, and the role of turbulent burst mechanisms that are common in mountain environments in generating shear stress to modify snow saltation. In doing so, the potential for adapting a continuum sand transport model for describing snow saltation particle motions is assessed.

2 Methods

Fieldwork was conducted during blowing snow events in March 2015 and February-March 2016 at the Fortress Mountain Snow Laboratory (FMSL), Kananaskis Valley, Alberta, Canada. FMSL receives at

Nik Aksamit 8/31/2016 2:41 PM
Formatted: Font:Not Italic

Nik Aksamit 8/31/2016 2:41 PM
Deleted: 2011,

Nik Aksamit 8/31/2016 2:41 PM
Deleted: from

Nik Aksamit 8/31/2016 2:41 PM
Deleted: to April 2015

least 800 mm water equivalent of snowfall each winter, can sustain wind speeds exceeding 35 m s^{-1} and is home to several well-instrumented high-altitude, wind-swept observation sites. The blowing snow site (2000 m.a.s.l.) was located in an open base area of the Fortress Mountain ski area (Fig. 1). The area was lightly used, allowing for a 350 m upwind fetch of undisturbed open snowfield, with the foot of a moderate ridge flanking the west 200 m away. The ground was snow-covered and shrub vegetation buried for the duration of the experiment with snow depths fluctuating from 60 to 120 cm. Two Campbell Scientific CSAT3 three-dimensional ultrasonic anemometers positioned at varying heights depending on snow depth on a single mast (10-40 cm and 140-200 cm) measured wind speed at 50 Hz in three axes.

The unique aspect of this experiment was the implementation of laser-illuminated high-speed videography for outdoor nighttime snow particle tracking observations. A portable rigid frame equipped with a Megaspeed MS85K high-speed camera and a 445 nm wavelength 1.5 W continuous-wave laser was situated on the snow surface less than 1 m downwind from the anemometer mast (March 23, 2015) or 33 cm away perpendicular to the flow (February 3, March 3, 2016). *Dennis and Nickels* (2008) suggest reasonable application of Taylor's hypothesis up to downstream distances of up to six times the boundary layer depth δ. While there are no measurements of δ for the present data set, it is safe to assume an extreme value of 1 m is less than 6δ which is often $\mathcal{O}(10-100\ m)$ in the Atmospheric Surface Layer (ASL). Thus, using Taylor's frozen turbulence hypothesis and mean wind speed of the two anemometers as a surrogate for convection velocity, the effect of the downwind separation on the representativeness of anemometer mast turbulence statistics for the actual location of snow transport is assumed negligible with lag times < 0.25 s. Similarly, for the crosswind orientation, the size of energy containing eddies (discussed in Section 3), even over short recordings, are large compared to the separation. Lags between instantaneous wind and particle velocities are mentioned in the Section 4.

The frame was positioned on the snow surface allowing the camera a perpendicular 30 x 140 mm view of the flow of saltating snow. Laser light was projected through a cylindrical lens to create a 2 mm wide plane orthogonal to both the snow surface and the view of the camera (Fig. 1). The light plane illuminated a 2D projection of saltating snow particles. This allowed recordings in the lowest 5 cm of the atmosphere, with minimal foreground shadowing and no background reflection. Particle Tracking

Nik Aksamit 8/31/2016 2:41 PM
Deleted: is

Nik Aksamit 8/31/2016 2:41 PM
Deleted: Figure

Nik Aksamit 8/31/2016 2:41 PM
Deleted: 70

Nik Aksamit 8/31/2016 2:41 PM
Deleted: (typically 40 and 200 cm)

Nik Aksamit 8/31/2016 2:41 PM
Deleted:

Nik Aksamit 8/31/2016 2:41 PM
Deleted: -Watt

Nik Aksamit 8/31/2016 2:41 PM
Deleted: , typically

Nik Aksamit 8/31/2016 2:41 PM
Deleted: .

Nik Aksamit 8/31/2016 2:41 PM
Deleted: mm

Nik Aksamit 8/31/2016 2:41 PM
Deleted: 10

Nik Aksamit 8/31/2016 2:41 PM
Deleted: .

Velocimetry (PTV) measurements were calculated by DaVis 8 (LaVision) software and estimated individual snow particle velocities using tracking algorithms that match discrete particles in subsequent frames imaged by the high-speed camera. Particle velocimetry techniques are normally used for wind tunnel studies (e.g. *Zhang et al.,* 2007; *Creyssels et al.*, 2009; *Ho et al.,* 2011, 2012; *Lu et al.,* 2012; *Tominaga et al.,* 2012; *Groot-Zwaaftink et al.*, 2014; *Paterna et al.*, 2016), with few applications, in any discipline, in an outdoor setting (e.g. *Morris et al.,* 2007; *Zhu et al.,* 2007; *Rosi et al.,* 2014; *Toloui et al.,* 2014). This is the first known application of PTV for boundary-layer blowing snow studies in a natural environment.

The high-speed saltation recordings provided a great degree of visual distinction of surface particle motion and the use of 2D laser illumination minimized particle overlap (e.g. *Kobayashi*, 1972). As the camera was focused close to the snow surface, hundreds of thousands of rebound and splash events were recorded over the winter field seasons. In addition to PTV, videos were later reviewed with playback reduced 40-70 times, providing qualitative insight to the mechanics of near-surface saltating particle motion and bed interactions.

Figure 2 displays an example of velocity vectors calculated from 1 second of 23 March 2015 (recording #3). The stationary snow surface was masked out. The dashed black line indicates the height (h_0) of the upper limit of particles whose velocities were heavily influenced by surface microtopography and contributed uncharacteristic velocity profile statistics. In order to account for gradual changes in surface topography, an orthogonal terrain following coordinate system such that $y = 0$ is always at the snow surface and the y-direction is parallel to gravity was adopted to calculate vertical profiles of mean projected horizontal particle velocity u_p, and particle number flux concentrations F_z.

$$F_z = \frac{n(z) * u_p(z)}{\sum_z \left(n(z) * u_p(z)\right)} \quad (1)$$

where $n(z)$ is the number of particles identified at height z. This allowed a consistent reference frame along subtle inclines like that found in Fig. 2. Immersed boundary coordinates based on the camera frame (x_f, y_f) are not representative of height above the complex surface, (e.g. $(x_f, y_f) = (5, 100)$ is below the surface whereas $(x_f, y_f) = (1, 5)$ is above the snow) and caused statistical values to become increasingly dubious as one approaches the roughness layer. This can result in misrepresenting surface

Nik Aksamit 8/31/2016 2:41 PM
Formatted: Font:Bold

Nik Aksamit 8/31/2016 2:41 PM
Deleted: provide

Nik Aksamit 8/31/2016 2:41 PM
Deleted: minimizes

Nik Aksamit 8/31/2016 2:41 PM
Deleted: season

Nik Aksamit 8/31/2016 2:41 PM
Deleted: video was

Nik Aksamit 8/31/2016 2:41 PM
Deleted: 100

Nik Aksamit 8/31/2016 2:41 PM
Deleted: ,

Nik Aksamit 8/31/2016 2:41 PM
Deleted: .

Nik Aksamit 8/31/2016 2:41 PM
Deleted: has been

Nik Aksamit 8/31/2016 2:41 PM
Deleted: are

Nik Aksamit 8/31/2016 2:41 PM
Deleted: contribute

Nik Aksamit 8/31/2016 2:41 PM
Deleted: (analogous marks exist

Nik Aksamit 8/31/2016 2:41 PM
Deleted: Figure 3). PTV vector fields

Nik Aksamit 8/31/2016 2:41 PM
Deleted: as this were used

Nik Aksamit 8/31/2016 2:41 PM
Deleted: (Fig. 3a-f)

Nik Aksamit 8/31/2016 2:41 PM
Deleted: , (Fig. 3g). The PTV region of interest was vertically partitioned into horizontal slices following a log-scale. This allowed particle bin sizes to remain consistent for velocity averages as particle number density exponentially decreased with height. In Fig. 3, the height of surface microtopography varies as recordings were made over hours of active erosion and deposition, changing the surface structure.

Nik Aksamit 8/31/2016 2:41 PM
Moved (insertion) [1]

fluxes. Additionally, the height of surface microtopography varied as recordings were made over hours of active erosion and deposition, changing the surface structure, and subsequently the relative height of measurements with an immersed coordinate system. Terrain-following coordinates allowed observations to be made over a natural snowpack, crucial for improving the realism of blowing snow measurements, while still accurately defining the near-surface region.

The improved realism afforded by PTV over a natural snowpack in the ASL was counterbalanced by increased difficulty in obtaining valuable data from this methodology and from sonic anemometry during blowing snow storms. Ultrasonic wind speed measurements sometimes included spikes, "NaN" readings or were flagged for skewness/kurtosis (*Vickers and Marht*, 1997); these concurrent video recordings were used only for qualitative comparison. Spanwise fluctuations in wind caused snow particles to travel transverse to the plane of light, and the streamwise wind direction usually varied at the blowing snow site over the course of an evening's observations. PTV relies on particles to remain in the plane of light for illumination and tracking through multiple frames. While the frame could be adjusted for slow variations in wind direction, directional variations during wind gusts were a significant complication. To reduce particle mismatch errors and improve velocity calculation accuracy, initial visual quality controls were implemented, discarding video that contained particles obviously moving transverse to the plane of light.

Post-processing required individual particles to be evident in at least five subsequent frames and limitations were imposed on velocity vector tracks to discard physically unrealistic acceleration or direction change from one frame to the next. The camera depth of field and light plane thickness limited out-of-plane particle velocity components to $\pm 0.5 ms^{-1}$. Further uncertainty derives from the limited ability of PTV software to match individual snow particles at high wind speeds (> 9 m s^{-1} at 40 cm height). The particle matching interrogation area becomes larger as wind speeds increase and particles travel further from one frame to the next. This exponentially increases the number of particles that may be incorrectly matched.

To verify particle enumeration, a dual-threshold black and white binarization technique adapted from *Otsu* (1979) was used to estimate particle concentration in each frame. This complimentary method of particle identification used algorithms that, unlike PTV, are not affected by transverse particle motion or

Nik Aksamit 8/31/2016 2:41 PM
Deleted: atmospheric boundary layer (ABL) is

Nik Aksamit 8/31/2016 2:41 PM
Deleted: Concurrent ultrasonic

Nik Aksamit 8/31/2016 2:41 PM
Deleted:

Nik Aksamit 8/31/2016 2:41 PM
Deleted: Upon

Nik Aksamit 8/31/2016 2:41 PM
Deleted: ,

Nik Aksamit 8/31/2016 2:41 PM
Deleted: were required

Nik Aksamit 8/31/2016 2:41 PM
Deleted: four

Nik Aksamit 8/31/2016 2:41 PM
Deleted: ; this reduced the number of video frames providing PTV

Nik Aksamit 8/31/2016 2:41 PM
Deleted: fields

Nik Aksamit 8/31/2016 2:41 PM
Deleted: 551,000 to 190,000, resulting in 560,000 snow particle velocity vectors calculated for 165 seconds of real time recording

Nik Aksamit 8/31/2016 2:41 PM
Deleted:

Nik Aksamit 8/31/2016 2:41 PM
Deleted: address this problem

Nik Aksamit 8/31/2016 2:41 PM
Deleted: single

Nik Aksamit 8/31/2016 2:41 PM
Deleted: (

Nik Aksamit 8/31/2016 2:41 PM
Deleted: ,

Nik Aksamit 8/31/2016 2:41 PM
Deleted: obtain measurements of the snow

Nik Aksamit 8/31/2016 2:41 PM
Deleted: pixel area

Nik Aksamit 8/31/2016 2:41 PM
Deleted: individual frames. The pixel area measurements

particle matching limitations in gusty conditions. Binarization estimates of blowing snow concentration profiles were in sufficient agreement with concentration profiles generated by PTV, lending confidence to the measurements of particle trajectories. Additionally, with the binary image and PTV time series, it was possible to use a flood-fill algorithm to identify the connected components of blowing snow particles. Making an assumption of grain sphericity and constant density ($917\ kg\ m^{-3}$) and using instantaneous mean particle velocities, the equivalent diameters of the particles were used to estimate blowing snow volume fractions and instantaneous density flux Q_s ($kg\ m^{-2} s^{-1}$). Particle diameter measurements generated gamma-distributions of particle size (Fig. 3) consistent with other blowing snow literature (*Budd,* 1966; *Schmidt*, 1982).

PTV measurements in exceptionally high wind speeds (> 10 m s^{-1}) were not possible because the laser light became blocked by particles. Therefore, the dataset used in this analysis is focused on observations taken during relatively low mean wind speeds for blowing snow, (mean $4 - 7\ m\ s^{-1}$, Table 2); these sometimes included periods of intermittent turbulent bursts and intermittent snow transport. After all post-processing, three nights of recording satisfied all quality controls requirements. This included twelve recordings spanning 266 seconds of raw video and 470,000 frames.

3 Results

Examination of data calculated from 23 March, 2015, 3 February and 3 March, 2016 demonstrated the value of PTV measurements over varying wind speeds during periods of natural variation in saltating grain shape, type, and size. Descriptions of the snowpacks following the designations of the International Classification for Seasonal Snow on the Ground (*Fierz et al.,* 2009) for each night can be found in Table 1, with particle size gamma distributions for each recording in Fig. 3. Sample videos from each night can also be found in the document supplement. During all three nights, transport was highly intermittent, implying wind speeds were near threshold conditions. This was a necessary condition for accurate particle tracking in aeolian systems as images can become easily saturated (*Ho et al.,* 2014).

Nik Aksamit 8/31/2016 2:41 PM
Deleted: tracking algorithm

Nik Aksamit 8/31/2016 2:41 PM
Deleted: .

Nik Aksamit 8/31/2016 2:41 PM
Deleted: qualitative

Nik Aksamit 8/31/2016 2:41 PM
Deleted: to lend

Nik Aksamit 8/31/2016 2:41 PM
Deleted: ,

Nik Aksamit 8/31/2016 2:41 PM
Deleted: ;

Nik Aksamit 8/31/2016 2:41 PM
Deleted: demonstrates

Nik Aksamit 8/31/2016 2:41 PM
Deleted: a period without significant changes in

Nik Aksamit 8/31/2016 2:41 PM
Deleted: or

Nik Aksamit 8/31/2016 2:41 PM
Deleted: Following the

Nik Aksamit 8/31/2016 2:41 PM
Deleted: 2009), saltating snow consisted of spherical graupel grains (mean diameter 413 μm) with many reaching 1000 μm in diameter. The bed was composed of 5 cm of fresh loose grains that had fallen the day of recording with a hand hardness index of 1 (Very Soft/Fist) over a supportive melt-freeze crust with no foot penetration. Snow

Nik Aksamit 8/31/2016 2:41 PM
Deleted: The small initial surface cohesion did not appear to be increased by any wind hardening during saltation. This not only minimized the influence of particle bonds on

Nik Aksamit 8/31/2016 2:41 PM
Deleted: transport dynamics but provided a plentiful upwind supply of loose snow grains. During this night the streamwise wind direction remained relatively consistent and parallel to the light plane, resulting in a relatively high number of snow particles velocities calculated per frame (up to 50

3.1 Wind Characteristics

Near-neutral (slightly stable) stability conditions were found during the entirety of the three nights of recording using flux and gradient based methods (document supplement Fig. 1-3), however, steady-state wind conditions $\left(\frac{\partial U}{\partial t} = 0\right)$ did not occur during the field campaign. The less strict steady-state requirements of *Foken and Wichura* (1996) were also tested to further confirm steady-state conditions were not evident. Recording and wind characteristics encompassing the three nights are displayed in Table 2. Fifteen minute and recording time period mean wind speed $\bar{u}$, friction velocity $u_*^2 = \left[\overline{u'w'}^2 + \overline{v'w'}^2\right]^{1/2}$ (*Stull*, 1988), and covariance based roughness length $z_0 = z\, e^{-0.4\bar{u}/u_*}$ are shown for both anemometer measurements as they are the parameters most often used in blowing snow models. Additional values of turbulence intensity, $I = \sqrt{\overline{u'^2} + \overline{v'^2} + \overline{w'^2}}/\sqrt{\overline{u^2} + \overline{v^2} + \overline{w^2}}$, and Shields number $S = \rho_{air} u_*^2 / \rho_{ice}\, g d$ (based on mean particle size for each video) over both time periods are provided, as well as mean blowing snow flux ($Q_s\ kg\ m^{-2} s^{-1}$) for the recordings.

If wind measurements are close to the surface, such as during the 3 March 2016 recordings, the physical path length of the sonic anemometers can result in losses of high frequency turbulence. Following the guidelines of *van Boxel et al.,* (2004), the Nyquist frequency (25 Hz) is a limiting factor for mean wind speeds greater than $3\ m\ s^{-1}$, and may also contribute to some discrepancy of low and upper anemometer turbulence measurements. Additionally, the lower anemometer measurements during Recording #2 on March 23, 2015 appears to have been contaminated as there is a significant change in covariance derived u_* and z_0 values between the two heights.

The ASL fit a Prandtl-von Kármán logarithmic-law profile poorly during the storms, most likely due to violations of horizontal-homogeneous-flat (HHF) terrain and stationarity requirements. Recording period log-law based roughness lengths $z_0 = e^{\frac{u_1 \ln(z_2) - u_2 \ln(z_1)}{u_1 - u_2}}$ and friction velocities $u_* = \frac{\kappa \bar{u}(z)}{\ln(z/z_0)}$ were loosely comparable to lower anemometer fluctuation-based measurements with z_0 errors less than $\pm$ 100% (except March 3 #9), and u_* errors less than $\pm$ 70%, often slightly underestimating.

The 15-minute roughness lengths that were generated by covariance methods resulted in inaccurate log-linear wind profiles that indicated a zero velocity zone for the wind well above the snow saltation layer

Nik Aksamit 8/31/2016 2:41 PM
Deleted: Neither

Nik Aksamit 8/31/2016 2:41 PM
Deleted: nor

Nik Aksamit 8/31/2016 2:41 PM
Deleted: occurred

Nik Aksamit 8/31/2016 2:41 PM
Deleted: recordings. As $\frac{\partial U}{\partial t} = 0$ is rarely satisfied in the ABL, the

Nik Aksamit 8/31/2016 2:41 PM
Deleted: ,

Nik Aksamit 8/31/2016 2:41 PM
Deleted: confirming

Nik Aksamit 8/31/2016 2:41 PM
Deleted: Wind

Nik Aksamit 8/31/2016 2:41 PM
Deleted: recording times on 23 March

Nik Aksamit 8/31/2016 2:41 PM
Deleted: 1

Nik Aksamit 8/31/2016 2:41 PM
Deleted: at 40 and 200 cm normal to the snow surface

Nik Aksamit 8/31/2016 2:41 PM
Deleted: However, the ABL did not fit a Prandtl-von Kármán logarithmic-law profile during the storm. Values of $\bar{u}$, u_*, and z_0 over the specific video recording times are also provided in parentheses. Along with

Nik Aksamit 8/31/2016 2:41 PM
Deleted: , comparing video recording-averaged (7.3 to 13.1 s) and 15-minute averaged values shows the influence of analysis timescale on characterization of wind flow. Turbulent gust-driven snow transport events dominated the night and these gusts are evident in the video recording timescale averages. However, increasing the timescale from ~10 s to 15-min averaging periods, as is often done in operational models, disguises these turbulent motions. Attempts to relate these values to blowing snow measurements are discussed below. ... [1]

Nik Aksamit 8/31/2016 2:41 PM
Formatted: Font:Not Italic

Nik Aksamit 8/31/2016 2:41 PM
Deleted: *Pomeroy* (2005). Using 15-minute periods to discretize the 23 March observatio ... [2]

Nik Aksamit 8/31/2016 2:41 PM
Deleted: transport for recordings #1 (Blue), #2 (Green), and #3 (Red), also designated by the ... [3]

Nik Aksamit 8/31/2016 2:41 PM
Deleted: u_p at specific heights for ascending particles in the three recordings, with error ba ... [4]

and often at extremes values of tens to hundreds of mm (Table 2). High roughness lengths appear characteristic of this mountain region. At a nearby site 14 km northeast and 600 m lower in elevation, *Helgason and Pomeroy* (2005) attributed similar large covariance derived z_0 values at varying heights to the effects of surrounding topography and the non-stationary and non-steady state nature of the wind. The modified "focal-point" log-linear wind profile proposed by *Bagnold* (1941) for aeolian transport did not show any improvements in describing this, providing focal lengths varying from several mm up to 6 m.

The wind was characterized by brief moments of intense gusting separated by periods of relatively calm conditions as also noted at the *Helgason and Pomeroy* (2005) research site. 15-minute turbulence intensity ranged from 26 to 113%. As a result, values of $\bar{u}$, u_*, and z_0 consistently differ between video recording-averaged (7.3 to 28 s) and 15-minute averaged values. Turbulent gust-driven snow transport events dominated the nights. 11 out of 12 fifteen-minute averages present lower wind speeds than the recording period with the long averages often below thresholds of transport.

Figure 4 shows varying Reynolds Stress ($RS = u'w'$) generation during each recording following the language of quadrant hole analysis (*Willmarth and Lu*, 1971). Sweep and ejection events (Q2 and Q4) often contributed the majority of RS at both anemometers, with a more pronounced role closer to the ground, indicating changes in the snow surface influence on wind mechanics. Q2 and Q4 stress also occupied a disproportionately small amount of time near the surface, as can be seen in the impact factors inset in the bar graphs ($IF = (\%\, Reynolds\ Stress)/(\%\, Time)$) that are greater than unity. Therefore, when strong events are captured during the recordings RS values can be much larger than long time averages. The presence of a single pronounced sweep event in Recording #3, March 23 (discussed more in Section 3.3) contributed to a high turbulence intensity (45%), and a much higher friction velocity than the fifteen-minute values (0.48 m/s and 0.24 m/s respectively) and will be discussed in detail in Section 3.3.

Understanding the changes in quadrants generating RS helps illuminate the differences in u_* values at the two measurement heights over these short recording timescales. The events with the largest discrepancy in u_* (besides March 23 #2 where low height wind measurements are questionable) are February 3 #3 ($u_* = \{0.30, 0.45\}\, m\, s^{-1}$) and March 3 #2 ($u_* = \{0.26, 0.43\}\, m\, s^{-1}$). This was the

result of a significant decrease in the magnitude of mean RS at the lower measurements (0.27 vs 0.11 $m^2\ s^{-2}$ and 0.22 vs 0.09 $m^2\ s^{-2}$, February 3 and March 3, respectively), while the turbulence intensity remained nearly constant (Table 2). The reduced presence of Q1 and Q3 at the lower heights, and increased impact factor of Q2 and Q4 (Fig. 4) indicated a complex shift in boundary layer dynamics towards the snow that is beyond the scope of this paper. Other recordings exhibited much closer friction velocity and roughness length values at the two anemometers, indicating similar turbulent motions were captured.

As also seen by *Bauer et al.* (1998), sweeps and ejections did not immediately follow one another, rather there were prolonged clusters of sweeps and ejections with gaps in between (Fig. 5a). The gaps may be a result of point measurements' inability to capture a full 3D motion (*Bauer et al.*, 1998), but nevertheless the measurements showed significantly different RS generation than that typically found in wind tunnels. For example, Fig. 5 a-b compares RS values in a recent blowing snow wind tunnel experiment of *Paterna et al.* (2016) with RS found on 3 February 2016 at FMSL at a similar friction velocity ($0.25\ m\ s^{-1}$ and $0.27\ m\ s^{-1}$, respectively). A sweep signal of magnitude greater than one standard deviation of RS is indicated above the given RS time series by a blue triangle, while similar ejections are marked by brown triangles. Visually, there is a noticeable shift toward clustered sweep and ejection events at FMSL (Fig 5a), in which clustered pockets of sweeps alternated with ejections, while the sweep/ejection cycle and turbulent energy occurred at much a higher frequency in wind tunnel-based measurements by *Paterna et al.* (2016) (Fig 5b). This is further confirmed in the power spectral density plots of streamwise wind speed (Fig. 5c), and in the discussion by *Paterna et al.* (2016). Reconciling these differences between motions in atmospheric and laboratory boundary layers is an open field of research (*Hutchins et al.*, 2012) and must be kept in mind when comparing blowing snow studies in indoor and outdoor environment, especially of radically different Reynolds number.

3.2 Vertical PTV Profiles

Figure 6 shows profiles of ascending particle horizontal velocity for the three nights of recording with linear regressions based on the lower 10 mm. Profiles were designated by their recording-specific low

anemometer u_* values, except for 23 March where the lower wind measurements for recording #2 were contaminated. Thus, 23 March recordings were compared by 2 m wind.

Particle motions began with an initial ejection velocity at the surface and then accelerate due to fluid drag in the wind. Therefore the height of an ascending saltating particle should be a function of the time spent accelerating. The profiles of horizontal velocities of ascending particles confirmed this acceleration in Fig. 6. The average momentum transfer from wind to grain was estimated from the inverse slope of the plots and indicated the ability of the wind to entrain and accelerate particles. For all three nights there is a near constant particle velocity gradient immediately above the surface, $\left(\frac{\partial u_p}{\partial z} = \gamma, \gamma \in \mathbb{R}^+\right)$. Above ~8-12 mm, depending on the night, mean particle velocities meander from the linear profile as seen in Fig. 6 and confirmed by normalized root mean square error (NRMSE) changes from the order of 0.01 to 0.1 above and below 10 mm, respectively. It must be noted, this did not indicate a discrete transition height from creep to saltation but is rather evidence of a continuous spectrum of particle velocities (*Anderson*, 1987; *Ho et al.*, 2012) transitioning to a higher energy population away from the surface. As these recordings captured intermittent transport, saltation is in constant readjustment to the turbulent wind, with particles falling in and out of the higher levels of saltation (discussed further in Section 3.3). This prevented a consistent adherence to the linear profile as seen by *Ho et al.* (2011), though both studies found linear profiles overestimate particle velocity at greater heights.

The velocity gradient (shear rate) γ, was estimated by linear regression and varied from $35 - 98\ s^{-1}$. Variations in wind speed and Q_s during each recording period indicate blowing snow transport never attained equilibrium. However, γ values are comparable to wind tunnel PTV sand velocity gradients ($39.0 - 150\ s^{-1}$) measured below 30 mm by *Zhang et al.* (2007), and the range $20 - 60\ s^{-1}$ found by *Ho et al.* (2011). For each night, γ increases with increasing friction velocity (Fig. 6d-f). The *Ho et al.* (2011) rigid bed experiments were conducted at comparable Shields numbers to the high HHI, wind-hardened February 3 experiments (Ho: [0.013, 0.043], Aksamit and Pomeroy: [0.026, 0.061]) and shared several trends discussed here and below. For example, as for *Ho et al.* (2011) the night of February 3 had on average the lowest γ values (mean $44\ s^{-1}$ versus $69\ s^{-1}$ for the erodible beds) and

Nik Aksamit 8/31/2016 2:41 PM
Deleted: begin

Nik Aksamit 8/31/2016 2:41 PM
Deleted: confirm

Nik Aksamit 8/31/2016 2:41 PM
Deleted: 3a, 3c, and 3e.

Nik Aksamit 8/31/2016 2:41 PM
Deleted: is

Nik Aksamit 8/31/2016 2:41 PM
Deleted: indicates

Nik Aksamit 8/31/2016 2:41 PM
Deleted: gusty periods

Nik Aksamit 8/31/2016 2:41 PM
Deleted: recordings

Nik Aksamit 8/31/2016 2:41 PM
Deleted: with height below 10 mm,

Nik Aksamit 8/31/2016 2:41 PM
Deleted: ; above this height,

Nik Aksamit 8/31/2016 2:41 PM
Deleted: are influenced by turbulence. The velocity gradient, γ, was estimated by

Nik Aksamit 8/31/2016 2:41 PM
Deleted: regression

Nik Aksamit 8/31/2016 2:41 PM
Deleted: 48.9, 51.6 and 94.0 ms^{-1}/m for recordings #1-3

Nik Aksamit 8/31/2016 2:41 PM
Deleted: , and is represented as the inverse slope of the plotted pink lines. These slopes are comparable to wind tunnel PTV sand velocity gradients ($39.0 - 150\ ms^{-1}/m$) measured below 30 mm by *Zhang*

Nik Aksamit 8/31/2016 2:41 PM
Deleted: . (2007).

Nik Aksamit 8/31/2016 2:41 PM
Moved up [1]: , (1)

Nik Aksamit 8/31/2016 2:41 PM
Deleted: The 10 mm transition corresponds with the upper extent of the low-energy population, where transport is characterized by tumbling, very short ballistic hops, and little influence from w'. This is also the region determined by *Creyssels et al.* (2009) and *Ho et al.* (2014) to be largely unaffected by increases in wind speed and is of critical importance for determining bulk flow properties from particle slip and ejection velocities, u_0 and v_0, respectively. While the 10 mm transition height witnessed in the field is lower than that found by *Ho et al.* (20 ... [5]

Nik Aksamit 8/31/2016 2:41 PM
Deleted: There is a maximum number flux ... [6]

the least variation in γ though transport occurred during comparable friction velocities, and higher Shields parameters than many March 23 and March 3 recordings (Table 2). The erodible bed studies were at significantly higher values for the Ho experiments (Ho: [0.07, 0.14], Aksamit and Pomeroy: [0.01, 0.11]), yet both studies also found increases in γ with friction velocity for the erodible beds. *Ho et al.* (2011) found less variance in γ over all friction velocities as could be expected from consistent equilibrium conditions.

As with wind tunnel sand studies (*Zhang et al.*, 2007; *Creyssels et al*., 2009; *Ho et al.,* 2011), large non-zero particle slip velocities were observed. The influence of surface microtopography and density of the flow prevented an exact measurement of particle slip velocity u_0, because it becomes difficult to enumerate all grains at the surface (*Creyssels et al*. 2009). However, extrapolating the linear regression plots of constant shear rate $du_p/dz = \gamma$ one can estimate u_0. As found in the same Ho study, our February 3 "rigid bed" experiments exhibited a nearly linear increase in u_0 with u_* (Fig. 6h). While our u_0 measurements had a larger range for the "erodible bed" nights of March 23 and March 3 (Fig. 6g, 6i) than that of *Ho et al*. (2011) and *Creyssels et al.* (2009) who found a near constant slip velocity, no definitive trend with u_* could be identified either. A purely constant slip velocity over erodible beds most likely depends on equilibrium transport conditions as has been theoretically explained by *Ungar and Haff* (1987) and may explain the ambiguity in our results.

Figure 7 shows the vertical profile of the normalized particle number flux calculated as Eq. (1). A normalized number flux profile was chosen instead of the volume fraction (e.g. *Ho et al.,* 2011) or mass flux density profile (*Creyssels et al.,* 2009) because of computational limitations of the PTV package in DaVis 8, and because of the non-equilibrium transport during the recordings. Since it is impossible to control the rate of transport in nature, and volume fractions will change with rates of transport, wind fluctuations and snow surface conditions, it was informative to compare number flux concentrations between periods of diverse mass transport to determine differing transport mechanics over varying snow and wind conditions. As the study was focused on the dynamic role of surface transport, and not measuring mass flux, we thus renormalized each concentration profile by the amount of flux that occurred during a recording to compare what proportion of total particle transport is occurring at each

height at suggested by *Ellis et al.* (2009) for aeolian transport profiles in nature. This allowed observation of changes in the relative importance of regions of transport.

The fractional number flux fits an exponential decrease of the form $\nu(z) = \nu_0 \exp(-z/l_\nu)$ with increasing accuracy as one approaches the densest flow at the surface, similar to sand and snow saltation profiles seen elsewhere (e.g. *Maeno et al.*, 1980; *Nishimura and Hunt*, 2000; *Creyssels et al.*, 2009; *Ellis et al.*, 2009; *Ho et al.*, 2011; *Lü et al.*, 2012), with ν_0 and l_ν being fitted parameters, the latter referred to as the decay length. The number flux decay length l_ν indicated how quickly the number flux concentration approached zero (Fig 7d-f), but because there were large variations in the surface concentration ν_0 in the present study, more consistent trends can be observed with the momentum deficit height h_ν, the height below which 75% of particle flux occured. As seen in the right inset of Fig. 7, there is a non-linear increasing relationship between friction velocity and h_ν for the February 3 and March 3 recordings. After disregarding March 23, (discussed below), values of h_ν followed an approximate power law relationship ($au_*^b + c, R^2 = 0.77$) with asymptotic-like behaviour towards the top of the region of interest (~11 mm). At low friction velocities, near-surface saltation was dominated by transport below 7 mm, with transport becoming gradually more uniform as h_ν approached the top of the camera frame at higher friction velocities.

March 23 exhibited very little change in h_ν and ν_0 with only a slight decrease in l_ν. Thus, concentration was largely invariant with wind strength. This is remarkably similar to the erodible bed findings of *Ho et al.* (2011). Only one recording had comparable Shields numbers to Ho, but the non-cohesive graupel bed, and spherical snow grains most similarly represented sand grains and an erodible sand bed out of the three nights.

The near surface location of the maximum of F_z found over all recordings in Fig. 7 is in disagreement with models using Bagnold's focal height (*Bagnold*, 1941) to predict a peak mass flux at some distinct height above the surface (e.g. *Pomeroy and Gray,* 1990). This stemmed from the earlier lack of high resolution measurements of near-snow surface processes outdoors, as results were in agreement with later wind tunnel observations (*Sugiura et al.*, 1998; *Nishimura and Hunt*, 2000) and numerical studies (*Nemoto and Nishimura,* 2004) of snow flux profiles as well as the recently measured blowing snow

Nik Aksamit 8/31/2016 2:41 PM
Deleted: stems

Nik Aksamit 8/31/2016 2:41 PM
Deleted: are

density profiles *Gordon and Taylor* (2009) and *Gordon et al.* (2009) found over natural snowcovers in Churchill and Franklin Bay, Canada, respectively.

For the time series under investigation, mean particle diameters had small temporal variance over any given recording (0.01 mm on Mar 23, 0.05 mm on Feb 3, and 0.02 mm on Mar 3). For a given time step, mean particle diameters tended to decrease with height in the field of view, typical of saltating snow studies (e.g. *Sugiura et al.*, 1998; *Gromke et al.*, 2014), with the most extreme variations on the order of 60 μm. From this it can be inferred that particle number concentrations were closely related to particle volume fractions through mean diameters, and can neglect variations in particle size with wind speed changes while admittedly underestimating the relative volume concentration close to the surface. Particles moving in the densest region of the flow, immediately above the surface, are in a zone where particle tracking by opto-electronic snow particle counters becomes impossible but PTV provides new information. Close to the surface, it is possible to observe the whole spectrum of saltating particle velocities including those considered to be moving via creep. Following the high and low-energy saltating grain populations theory of *Ho et al.*, (2014), a terrain following height bands were chosen such that two end-case populations could be delimited. Using a height separation of 3 mm for three low wind speed recordings (23 March #2 and 3 March #1 & 4) and 4 mm for all others, Fig. 8 displays horizontal velocity histograms for descending snow grains above and below these designations. For every night there was a denser surface flow whose mean statistics are dominated by slow moving particles. This is to be expected from the particle velocity and number flux profiles in Fig. 6 and 7. Transitioning away from the densest flow, the upper region histograms show saltating particles have already begun to transition towards a higher energy population, with transport dynamics centred around larger horizontal velocities resulting in a higher mean. The increasing proportion of high-energy particles with distance from the surface was due to the need for a greater velocity to reach greater heights on a ballistic trajectory from the surface and the subjection to stronger winds with increasing distance above the surface.

What is of most interest here is that a separating height was chosen such that for each recording the two histograms begin to agree for the highest energy grains (Fig. 8). That is, the highest energy population of descending particles present in the upper band can also be identified in the surface flow and that high

Nik Aksamit 8/31/2016 2:41 PM

Deleted: Projected horizontal velocity histograms for descending particles in Fig. 3h for the near-surface and upper layers of Rec. #3 ($u_* = 0.57\ ms^{-1}$) help illuminate the shift in snow transport mechanics when transitioning to particles in the tail of the particle velocity distributions (*Ho et al.*, 2012). Particle vectors below 1 mm were discarded to eliminate very small velocities from shaking surface particles that do not contribute to the blowing snow flux. Particle velocity vectors within a 4 mm neighborhood of the surface microtopography are in "near-surface region" where a dense flow of short hops dominates. Particles from 4 to 30 mm above the surface determine the "upper layer", where particles capable of splash dominate. Fig. 3h confirms that the near-surface region is dominated by low velocity particles, which are relatively rare in the upper layer. However, the ratio of particles counted in near-surface to the upper regions declines as particle velocity increases, dropping to less than 1 above $u_p = 2\ ms^{-1}$. The dashed line in Fig. 3h displays the difference between the near-surface and upper region histograms. There are 17% more descending particles with velocity $u_p \geq 1.7\ ms^{-1}$ in the upper region compared to the near-surface layer. Because this histogram details only descending particles, the similarity in particle counts implies the near-surface measurements include splashed and tumbling surface gains as well as high-energy particles descending from the upper region. ... [7]

and low-energy populations coexisted as part of a continuous spectrum of motion at the surface. This was indicative of an inherent coupling of the creep and saltating grains. Working with the assumption that the surface histograms contain contributions from both the high and low-energy populations of grains, whereas the upper band histogram consists only of high-energy grains, we can then identify the low-energy population at the surface as the difference of the two collections of particle vectors. With this, we can begin to quantify the role that creep plays in surface impact and wind momentum balance. Note, identifying creep particles is only possible when using both the particle velocity and location because high-energy grains were also impacting surface. The difference of surface and upper region populations showed a low-energy near-surface population that constituted 44-52%, 21-29% and 37-61% of the number flux on March 23, February 3, and March 3 respectively. Thus the slow moving low-energy creep grains were a considerable contribution to total particle flux below 20 mm over all snow types and wind conditions observed.

In the near-surface region, the ability of the snowpack to redistribute impact momentum was estimated from PTV data derived from each recording. Snow particle rebound efficiency varied from night to night, and was quantified by the restitution coefficient, $\overline{e_{xz}} = \overline{\|s_r\|}/\overline{\|s_i\|}$, where $\overline{\|s_r\|}$ and $\overline{\|s_i\|}$ are mean ejection and impact speeds of particles, respectively, at 6 mm $\pm$ 2 mm such that the lower bound of the measurement band corresponds with the upper bound of the surface band generating Fig. 8 histograms. Because of the density of the particle flow, and transverse components of travel, a bulk statistical approach must be used to quantify momentum redistribution into the particle bed. Therefore particle ejection speeds of both the rebounding grains and the splashed grains that reach ~20 particle diameters above the surface were averaged. Over the course of the campaign, $\overline{e_{xz}}$ varied from 0.58 to 0.84, within the bounds of the previous wind tunnel blowing snow study of *Sugiura and Maeno* (2000) who used a complimentary particle by particle approach, separating individual rebounding and splashed grains. The mean restitution coefficient was 0.69 for the graupel grains on March 23, 0.79 for fresh snow on March 3, and 0.73 for old snow on February 3. This suggests rebound efficiency was dependent on time-sensitive saltating snow crystal and bed mechanical/material properties, as also noted in a blowing snow wind tunnel study by *McElwaine et al.* (2004).

Using $\overline{e_{xz}}$ from each recording and assuming a constant mean grain diameter, it was then possible to

sum the total impacting high-energy snow grain momentum and to estimate how much momentum was lost to the snow bed through surface bond breaking, particle shattering or particle ejection. Similarly, one can determine the amount of momentum present in the low-energy surface population. Consistently, there was a large residual in the momentum balance, with up to 10 times the momentum in the low-energy surface particles than that which was available from particle impacts. This ratio of the sum of momentum in the creeping population to that lost to the surface from impacting high-energy particles capable of splash is indicated on each recording histogram in Fig. 8 as "Crp/Spl". All coefficients greater than one indicate a creep layer with total momentum greater than that which was possibly gained through saltating particle impacts. The creep layer was not merely a region of splashed grains that balances the momentum lost from saltating particles, but also behaves as a sink of wind momentum as well, further complicating the lower boundary layer condition for wind models.

3.3 Turbulent Event Transport

The initiation mechanisms observed at the surface during the onset of transport events differ from those proposed in single threshold velocity models (e.g. *Schmidt*, 1980), suggesting multiple thresholds with the dense surface flow playing a crucial role. All three transport thresholds recognized during video playback are crossed during 23 March recording #3 (Fig. 9) where an isolated gust was captured with minimal antecedent transport. Thus, it will be used as an example for further discussion. Concurrent streamwise wind measurements at 200 and 40 cm are plotted in Fig. 9a showing penetration of a turbulent sweep to the surface that is responsible for snow transport. In Fig. 9a, filled circles indicate sweep events with RS exceeding one standard deviation of total RS (colors corresponding to measurement heights), while triangles indicate similar moments of strong ejections. Fig. 9b and 9c show time series of spatially averaged particle velocities, and total particles tracked, respectively, in three height bands, $1 < z < 4\ mm$ (Near-Surface), $4 \leq z < 8\ mm$ (Mid), and $8 \leq z < 30\ mm$ (High). These three heights were chosen to demonstrate the subtle differences in particle transport and the continuum of motion as grains began motion and began bouncing to greater heights as wind speeds increased. These are not hard thresholds of "creep" versus "saltation" regimes. Fig. 9d shows the time series of instantaneous blowing snow flux Q_s in $kg\ m^{-2}s^{-1}$. These binarization based flux

Nik Aksamit 8/31/2016 2:41 PM
Deleted: Figure 4).

Nik Aksamit 8/31/2016 2:41 PM
Deleted: 4a

Nik Aksamit 8/31/2016 2:41 PM
Deleted: initiates

Nik Aksamit 8/31/2016 2:41 PM
Deleted: Figs. 4b

Nik Aksamit 8/31/2016 2:41 PM
Deleted: 4c

Nik Aksamit 8/31/2016 2:41 PM
Deleted: 4d

Nik Aksamit 8/31/2016 2:41 PM
Deleted: the number of pixels occupied by snow crystals in each frame, determined with the *Otsu* (1979)

Nik Aksamit 8/31/2016 2:41 PM
Deleted: method mentioned above. Pixel area

measurements compliment PTV calculations in intense gusting when enumerating all particles through tracking became difficult.

At the end of a strong ejection event (2.5-4.5 s) at wind speeds near $4\ m\ s^{-1}$, snow particle motion began with tumbling surface movement where aerodynamic drag was barely able to directly break weak surface crystal bonds and initiate rolling (5 s in Figs. 9b-d). Particle-bed collisions were concurrently responsible for breaking surface snowpack matrix structures at these wind speeds, though were not yet able to initiate a splash regime. The supplementary video for March 23 begins at 5 seconds in this time series. The bonds broken by low-energy grains at low wind speeds enabled more grains to be freely available for entrainment. During this time, horizontal particle velocities remained low and in the near surface region (Fig. 9b), with no particles being tracked above 4 mm (Fig 9c), and total mass transport remaining low (Fig 9d). At this stage, the only particles in motion were those classically termed creep.

As the wind speed increased (> 6 s), another threshold was crossed ($\sim 4.5 - 5\ m\ s^{-1}$) above which tumbling near-surface particles were sufficiently accelerated so that they could regularly bounce off the uneven surface and out of the creep layer. This initiated what is classically described as saltation, evidenced by the increasing presence of particles tracked in the "Mid" and "High" regions in Fig. 9c (above 4 mm), though snow mass flux remained moderate at this time (Fig 9d). A continuum of motion is evidenced here as all mean particle velocities increased and velocities steadily increased away from the surface.

At 8 s, a strong sweep is present at 2 m that penetrates to the surface by 8.5 s when the last critical wind velocity threshold was crossed ($\sim 6\ m\ s^{-1}$); that at which saltating particles were sufficiently accelerated to initiate an active splash regime upon rebounding. At this point snow mass flux increased exponentially (Fig. 9d), abruptly saturating the recording frame with snow particles and limiting illumination for successful PTV (discussed below). Similar exponential increases of sand flux during gust onset and splash commencement have been documented (*Willetts et al.*, 1991). The increased snow mass flux (Fig 9d) persisted for the duration of the gust, (until 10 s) after which both high and low streamwise velocities decreased. From 11 s onwards, the decreasing wind speed was no longer able to sustain the mass transport and particle counts dropped in the "Mid" and "High" regions of flow. A

Nik Aksamit 8/31/2016 2:41 PM
Deleted: as a snow flux index …hen indivi ... [8]

Nik Aksamit 8/31/2016 2:41 PM
Deleted: beginning…nd of the turbulent sw ... [9]

Nik Aksamit 8/31/2016 2:41 PM
Deleted: at wind speeds …here aerodynan ... [10]

Nik Aksamit 8/31/2016 2:41 PM
Deleted: , it crossed a

Nik Aksamit 8/31/2016 2:41 PM
Deleted: appearance…ncreasing presence ... [11]

Nik Aksamit 8/31/2016 2:41 PM
Deleted: penetrated…s present at 2 m that ... [12]

Nik Aksamit 8/31/2016 2:41 PM
Deleted: are…ere sufficiently accelerated ... [13]

Nik Aksamit 8/31/2016 2:41 PM
Moved down [2]: The role of sweep events such as this for initiating snow saltation are potentially important for developing models that couple turbulence to snow erosion, entrainment and mass flux and may help resolve current uncertainty in estimating threshold conditions for transport.

Nik Aksamit 8/31/2016 2:41 PM
Formatted: English (US)

Nik Aksamit 8/31/2016 2:41 PM
Deleted: pixel area values …ass flux (Fig ... [14]

combination of inertia and wind drag prolonged transport in the creep layer, maintaining rolling crystals that continued breaking surface bonds and were available for transport during the next gust.

High region particle velocity spikes occurred with some delay after 8.5 s due to the intense snow particle density blocked the laser light illumination, making particle tracking difficult. At 9 s, the number of particles tracked in the upper region increased as particles tracked near the surface decreased. This is likely a measurement error due to the dense granular flow attenuating light penetration to the snow surface. As the gust began to subside after 9 s, PTV-observed velocities and particle numbers increased because tracking became more successful. Then, as wind speed decreased further, observed velocities and particle numbers decreased as expected. The *Otsu* (1979) binarization thresholds were determined over short sub-periods (0.085 s) of recording #3 (Fig. 9d), allowing the thresholding technique to adapt to different levels of illumination and overcome these saturation issues.

Particle impact dynamics evolved as snowpack surface conditions varied during the season with multiple melt-freeze cycles, periods of wind hardening and the appearance of mixed grain types. Warm (Air Temp: +1°C) February 2015 snowstorms precipitated enormous aggregate and rimed crystals that expanded the role of near-surface particle dynamics. Large (4 mm diameter) tumbleweed-like aggregate grains termed here "tumblons", eroded many smaller crystals from the surface or shattered themselves and immediately became saltating grains, depending on impact velocity. Overlain PTV vectors can be seen in Supplementary Video – Tumblon PTV, where an impacting tumblon shatters at the surface at seven seconds, with an impact velocity of approximately $(u, v) = (2.46, -0.43)\ m\ s^{-1}$. At 35 seconds in the PTV video, a comparably sized tumblon with velocity $(u, v) = (0.6, 0.1)\ \mathrm{m\ s^{-1}}$ tumbles across the screen without collapse. This type of particle motion has not been described before and would seem to be a distinctive feature of blowing snow during or shortly after snowfall of large dendritic flakes in relatively warm conditions. Uniquely large grains can also be found in the March 3 supplementary video, though shattering dynamics do not appear prevalent on that night as large grains resulted from riming and not wet grain aggregation. Decomposing and aggregate grains of extreme size have not been reported for saltating sand. This may limit the application of sand bed momentum balances and wind tunnel studies where there are no contributions of falling snow to saltation.

Nik Aksamit 8/31/2016 2:41 PM
Deleted: in the PTV time series, but

Nik Aksamit 8/31/2016 2:41 PM
Deleted: subsided

Nik Aksamit 8/31/2016 2:41 PM
Deleted: 4d

Nik Aksamit 8/31/2016 2:41 PM
Deleted: Analyzing the instantaneous wind signal in Fig. 4a helps explain the source of the fastest moving particles in recording #3. A single turbulent sweep event ($u' > 0, w' < 0$) from 8 to 9 s generated considerable Reynolds stress

Nik Aksamit 8/31/2016 2:41 PM
Moved down [3]: ; this turbulent structure is widely reported to be involved in initiating aeolian sediment transport (*Grass,* 1971; *Jackson*, 1976; *Sterk et al.* 1998; *Chapman et al.,* 2012).

Nik Aksamit 8/31/2016 2:41 PM
Deleted: This 1 s sweep accounted for 29% and 25% of total absolute Reynolds stress at 40 and 200 cm, respectively, and contributed 56% of total snow particle flux below 30 mm, but only occupied 8% of the time. Turbulent ejections ($u' < 0, w' > 0$) generated 39% of total absolute shear stress during the recording and contributed the same direction of Reynolds stress values to friction velocity calculations but only resulted in 3% of total snow particle flux. This distinction in turbulent sweeps and ejections explains the diminished efficiency of ejections to generate saltation alluded to in section 3.1 with respect to Rec. #1.

Nik Aksamit 8/31/2016 2:41 PM
Moved down [4]: Varying the lag time between wind and snow measurements from 0 to 1 second to determine the resultant snow flux had no significant effect on these calculations.

Nik Aksamit 8/31/2016 2:41 PM
Deleted: . ... [15]

Nik Aksamit 8/31/2016 2:41 PM
Deleted: (+

Nik Aksamit 8/31/2016 2:41 PM
Deleted: (Figure 5).

Nik Aksamit 8/31/2016 2:41 PM
Formatted: Font:Times, 10 pt, Italic, Font color: Accent 2, English (UK)

Nik Aksamit 8/31/2016 2:41 PM
Deleted: and

Nik Aksamit 8/31/2016 2:41 PM
Deleted: that do not include

Nik Aksamit 8/31/2016 2:41 PM
Deleted: modeling saltating snow in natural conditions

4 Discussion

Choosing the appropriate timescale to characterize turbulent energy for snow transport is vital. From Table 2 and Fig. 6 & 7, it is clear that recording specific particle velocity gradients $\frac{\partial u_p}{\partial z}$, and flux concentration profiles did not scale with 15-minute u_* or z_0 values as is assumed on average for many existing snow saltation models (*Pomeroy and Gray*, 1990). Part of this lack of concurrence was due to intermittent transport and large-scale atmospheric motions generating high shear over short periods (Fig. 4). Also, the limited Reynolds numbers possible in wind tunnel blowing snow experiments cannot replicate the complex eddy structure of the ASL. Thus kinetic energy is contributed to mass transport at much higher frequencies in wind tunnels (*Paterna et al.*, 2016) and the full spectrum of motion can be measured over shorter time scales. Moreover, with the influence of surrounding topography, capturing the relevant range of energy containing eddies to predict snow transport in the alpine is less straightforward. The 15-minute mean wind speeds were often below any snow transport thresholds reported in the literature (*Li and Pomeroy*, 1997). The significant errors arising when applying time-averaged values in a u_* driven transport model (i.e. *Bagnold*, 1941) in intermittent winds have been well examined for sand (*Sorenson*, 1997) and equally apply for snow saltation. *Pomeroy and Li* (2000) accounted for the inapplicability of steady-state theory in near threshold conditions by using a probability of occurrence function to reduce transport fluxes at lower mean wind speeds, but it is unclear whether this empirical correction can account for the complex interaction of turbulence and particle flux near the threshold. Disagreements between u_* and z_0 values at the two measurement heights, large 15-minute z_0 values, and disagreement between log-law based and covariance generated u_* values reinforces the notion that all required assumptions must be met before log-law profiles should be applied for blowing snow models (*George*, 2007), especially in complex terrain.

Blowing snow PTV transport profiles were clearly more related to recording-specific u_* than 15-minute values because of the non-steady state nature of the wind. As found in several wind tunnel sand studies (*Creyssels et al.*, 2009; *Ho et al.*, 2011), particle velocity gradients adhered to linear profiles below ~8-12 mm depending on the night. The low-energy creep population of particles near the surface were less affected by fluctuations in wind strength (*Ho et al.*, 2014), which resulted in more temporally consistent

Nik Aksamit 8/31/2016 2:41 PM
Moved down [5]: This is the first investigation to measure outdoor snow particle flux and velocity immediately above the snow surface.

Nik Aksamit 8/31/2016 2:41 PM
Deleted:

Nik Aksamit 8/31/2016 2:41 PM
Moved down [6]: It provides an opportunity to test certain observations of saltating particle flux trajectories measured in wind tunnels. Though observations were restricted to moderate wind speeds and intermittent transport, they show the importance of creep to blowing snow transport initiation and transition to full saltation. Being able to relate high frequency turbulent wind speed to snow transport (e.g. *Guala et al.*, 2008) is cr... [16]

Nik Aksamit 8/31/2016 2:41 PM
Deleted: 1

Nik Aksamit 8/31/2016 2:41 PM
Deleted: 3

Nik Aksamit 8/31/2016 2:41 PM
Deleted: short timescale PTV maximums of u_p,

Nik Aksamit 8/31/2016 2:41 PM
Deleted: do

Nik Aksamit 8/31/2016 2:41 PM
Deleted: $u_{*_{15}}$

Nik Aksamit 8/31/2016 2:41 PM
Deleted: $z_{0_{15}}$

Nik Aksamit 8/31/2016 2:41 PM
Deleted: . For example, the highest velocit... [17]

Nik Aksamit 8/31/2016 2:41 PM
Moved down [7]: the need to account f... [18]

Nik Aksamit 8/31/2016 2:41 PM
Deleted: 2014).

Nik Aksamit 8/31/2016 2:41 PM
Deleted: is

Nik Aksamit 8/31/2016 2:41 PM
Deleted: .

Nik Aksamit 8/31/2016 2:41 PM
Deleted: well

Nik Aksamit 8/31/2016 2:41 PM
Deleted:

Nik Aksamit 8/31/2016 2:41 PM
Deleted: The recording-specific log-law w... [19]

Nik Aksamit 8/31/2016 2:41 PM
Deleted: (i.e.

Nik Aksamit 8/31/2016 2:41 PM
Deleted:).

periods of near surface low-energy transport and lower NRMSE values. Recent blowing snow wind tunnel experiments found log-linearity present in the horizontal velocity profile (*Tominaga et al.*, 2013), though this was not observed in the present study because of a lack of presence of a log-law for the wind.

For all recordings, the velocity gradients γ increased with increasing friction velocity estimates (Fig. 6d-f). Thus even in the dense low-energy population of grains, there was noticeable adaptation to changing wind speeds. However the role of low-energy grains diminished as surface grains became less available with increasing surface hardness. As with the rigid bed experiments from *Ho et al.*, (2011) at similar Shields parameters, there was a much smaller variability in γ for the wind-hardened bed on February 3 than for the two nights with lower HHI, with lower γ values over all. The momentum deficit height h_v was also highest for February 3 (Fig. 7 inset) with relatively low Shields numbers (0.026-0.061), indicating a muted role of creep and a more uniform saltation layer.

On the same night, a linear increase in particle slip velocity u_0 was observed for wind-hardened beds, further mimicking some of the findings of rigid beds for *Ho et al.*, (2011). This showed a general acceleration of all grains in saltation when there are fewer new grains to be entrained in the flow. In comparison, there was much less variability for slip velocity for March 23 and March 3 over a wider range of Shields parameters and no clear increasing or decreasing trend. A constant slip velocity is characteristic of erodible beds in equilibrium sand transport experiments (*Creyssels et al.*, 2009, *Ho et al.*, 2011). Presumably, as increasing concentration compensates for increasing friction velocity, u_0 returns to mean values over time. The snow transport observed was in constant readjustment to changes in wind speed, and equilibrium was never reached in the experiments, though smaller changes in u_0 may be indicative of early stages of the equilibrium process as theorized by *Ungar and Haff* (1987).

Particle number flux concentration profiles were fit to an exponential decrease model with increasing accuracy as one approached the consistent dense flow at the surface, as predicted in many other sand and snow studies (*Maeno et al.*, 1980; *Nishimura and Hunt*, 2000; *Creyssels et al.*, 2009; *Ellis et al.*, 2009; *Ho et al.*, 2011; *Lü et al.*, 2012). A direct comparison of decay length (l_v) between recordings and other experiments was impractical because large variations in surface concentration (ν_0) skewed decay length as an analog for saltation height. Instead, it was found that momentum deficit height h_v increased

for most recordings with increasing friction velocity. Low h_v values imply the majority of particle transport momentum is present near the surface. The presence of low-energy near-surface particles at lower friction velocities behaved as a reservoir for the transition to saltation with subsequent increases in wind speed. As wind accelerates, more particles are readily transported to upper heights and accelerated, vertically distributing the mass flux more uniformly. Increasing h_v values with u_* support a decreased role of creep in the near-surface mechanics. This occurs gradually with increasing wind speed, rather than involving discrete transport threshold velocity values for separate modes of transport. The notable exception for this trend in h_v was the night of March 23 (Fig. 7, inset – red dots) where h_{v_2} l_{v_2} and v_0 values remained constant as was predicted by *Ho et al.* (2011) for erodible beds. This difference in behaviour can be physically justified as for spherical graupel grains over a non-cohesive bed, the conditions most closely resembled sand, and so the number flux profiles behaved more similarly to sand than for the other two nights of blowing snow.

Histograms of horizontal velocity further supported the relevant and dynamic role of the low-energy surface population of blowing snow (Fig. 8), and the decreasing importance of near-surface mass flux with increasing surface hardness. Uniformly, there is an imbalance of momentum lost by impacting high-energy grains and that found in the creep layer. This created a requisite wind to creep momentum transfer that is much more substantial over erodible beds. The ratio of particle momentum in creep to that which was contributed by splash is much higher over erodible beds with lower HHI (March 23 and March 3) than on the wind hardened rigid bed night of Februrary 3 (4-10 versus 2, Fig. 8). This complimented the fact that the low-energy surface transport on February 3 had the smallest contribution to total number flux. Thus particle type and snow bed properties played a significant role in the surface momentum balance, changing the uniformity of saltation profiles and wind momentum lost directly to creep. For the erodible bed recordings (March 23, 2015 and March 3, 2016), the momentum present in the slow surface transport was often larger than that found in the upper region high-energy grains as can be seen by Crp/Spl > 4. For events with larger grains and lower surface hardness, transport initiation dynamics changed as wind played a larger role than splash in generating creeping particles. Mean particle diameters remained relatively similar over all recordings and thus transport initiation functions

need to account for snow bed hardness or erodibility as there is a connection to entrainment versus splash contributions.

Analyzing the instantaneous wind speeds in Fig. 9a helps to explain the short timescale roles of gusts, high friction velocity and turbulence intensity for snow transport in recording #3. The turbulent sweep event ($u' > 0, w' < 0$) from 8 to 9 s generated considerable RS; this turbulent structure is widely reported to be involved in initiating aeolian sediment transport (*Grass*, 1971; *Jackson*, 1976; *Sterk et al.* 1998; *Chapman et al.*, 2012). This 1 s sweep accounted for 29% and 25% of total absolute RS at 40 and 200 cm, respectively, and contributed 56% of total snow particle flux below 30 mm, but occupied only 8% of the time. Turbulent ejections ($u' < 0, w' > 0$) generated 39% of total absolute shear stress during the recording and contributed the same direction of RS values to friction velocity calculations but only resulted in 3% of total snow particle flux. Varying the lag time between wind and snow measurements from 0 to 1 second to determine the resultant snow flux had no significant effect on these calculations.

In this gusty alpine environment, periodic turbulent gusts generated the majority of momentum flux as seen by Impact Factors greater than unity at the surface for Q2 and Q4, and small contributions from Q1 and Q3 (Fig. 4). More importantly, recording #3 showed that the sweep event with strong positive u' fluctuation resulted in particle entrainment and transport, whereas the large ejection event was ineffective at generating blowing snow. As suggested by *Sterk et al.* (1998), instantaneous wind speed is a potentially better predictor of snow transport than friction velocity. However, during each night, the mass flux for each recording scaled with increasing friction velocity (Table 2). This resiliency may help explain some of the robustness of u_*-based time-averaged uniform trajectory blowing snow models, but requires further investigation. The role of sweep events such as this for initiating snow saltation are potentially important for developing models that couple turbulence to snow erosion, entrainment and mass flux and may help resolve current uncertainty in estimating threshold conditions for transport. The importance of understanding snow response to instantaneous wind speed is further increased in complex terrain where the 300 m of clear upwind fetch or 60 s of constant wind suggested by *Takeuchi* (1980) for saltation to fully develop is not always available. For a more general application, this requires further investigation of turbulent snow transport over longer time series and other snow conditions.

Nik Aksamit 8/31/2016 2:41 PM
Moved (insertion) [3]

Nik Aksamit 8/31/2016 2:41 PM
Moved (insertion) [4]

Nik Aksamit 8/31/2016 2:41 PM
Deleted: Steady-state equilibrium saltation models (e.g. *Pomeroy and Gray*, 1990; *Doorschot and Lehning*, 2002) are inappropriate for these situations, with further complications arising from the varying mechanics of transport during gusts, as seen in recording #3. Over short recording periods of less than 10 s, with hundreds of thousands of particle velocity vectors, there are still large standard deviations around mean snow particle velocities (Fig 3). Analysis of recording #3 indicates that there is large variability in snow transport mechanics, with concentration profiles, particle velocities, and saltation height changing over short time scales. This variability appears largely part due to high frequency particle-turbulence interactions and frequent surface impacts. ... [20]

Nik Aksamit 8/31/2016 2:41 PM
Deleted: and $u' > 0$ events disproportionately accounted for snow transport.

Nik Aksamit 8/31/2016 2:41 PM
Deleted: more indicative

Nik Aksamit 8/31/2016 2:41 PM
Moved (insertion) [2]

Nik Aksamit 8/31/2016 2:41 PM
Formatted: English (US)

Designating creep as distinct from saltation as originally done by *Bagnold* (1941) is not only unnecessary but physically inaccurate as snow transport displays a continuous spectrum of motions, similar to that proposed for sand by *Anders*on (1987), and individual particles can easily transition from one form of motion to another over their trajectories. However, two populations in this spectrum were identified in the analysis of Fig. 6-9. While undergoing windspeed fluctuations, the region of near-surface flux has the most temporally consistent transport (Fig 9). This was also the region of highest velocity variance (Fig. 8), yet the consistent presence of the slow particle flow allowed the best fit of particle number flux and mean particle velocity to profiles suggested in the equilibrium sand transport literature. The worst fit of both gradients always occurred at the upper parts of the video frame, the region dominated by high-energy particles (Fig. 8). These high-energy particles constituted the population of fast moving grains that was most susceptible to changes in wind speed (*Ho et al.* 2014) and most temporally intermittent (Fig. 9).

In previous work, a 10-20 mm transition in flux dynamics was exhibited by a change in particle blowing snow density formulae (*Gordon et al.*, 2009) and blowing sand mechanics. Utilizing simultaneous PIV and PTV to obtain two-phase (sand-wind) wind tunnel velocity measurements, *Zhang et al.* (2007) also found a comparable, extremely dense surface flow below this height. Of note, the wind was significantly modified below 15-20 mm for *Zhang et al.* (2007) in the presence of saltating particles with a shallower convex wind velocity gradient, due to particle momentum extraction in the near-surface region as predicted by Bagnold's focus height (*Bagnold*, 1941). The role of creep in this wind momentum deficit appeared significant and temporally variable.

The creep layer has proven to be a critical and readily available reservoir of tumbling particles during the onset of saltation. The lower boundary condition for momentum transfer is complex due to creep and dependent on instantaneous wind speed and turbulent motions near the surface. As a result, equilibrium conditions were never achieved. Non-equilibrium saltation-wind interactions cannot be described with simple uniform trajectories. The majority of particle trajectories in saltation consist of short hop lengths and times, resulting in high frequencies of particle collisions that break surface bond structures, and create dense quasi-fluidized bed characteristics. The complexity of conservation of mass, momentum, and kinetic energy in blowing snow in natural environments, such as measured here, cannot

Nik Aksamit 8/31/2016 2:41 PM
Deleted: However, two populations in this spectrum can be delimited by trends in Fig. 3 subplots at $u_p = 1.7\ ms^{-1}$. In Fig. 3h, $x = 1.7$ coincides with the convergence of upper and lower layer particle count histograms and identifies the high-energy particles descending through both layers. In Fig. 3e, the u_p plot crosses $u_p = 1.7\ ms^{-1}$ near $z = 10$ mm, the height below which 99% of particles are tracked and above which particle concentrations remain similar with height (Fig 3g). This change in gradient is suspected to correspond with the diminishing frequency of surface impacts and prolonged wind acceleration.

Nik Aksamit 8/31/2016 2:41 PM
Deleted: has also corresponded with a

Nik Aksamit 8/31/2016 2:41 PM
Deleted: Quantifying transitions that relate particle energy to characteristics of motion and wind response may help to better couple classic saltation models with creep boundary conditions or inform new saltation models that include the full range of initiation mechanism dynamics

Nik Aksamit 8/31/2016 2:41 PM
Deleted: Though the importance of near-surface motions at higher wind speeds in natural conditions remains unclear, the

Nik Aksamit 8/31/2016 2:41 PM
Deleted: are

be understated, especially when the large rimed, aggregate tumblons were present. In the alpine snowpacks investigated, variable particle restitution coefficients contributed to this complexity. While high HHI wind-hardened surfaces exhibited similar behaviour of slip velocity and particle velocity gradients as rigid bed sand studies, complexities over a natural snowpack prevented conclusive bimodal "erodible" versus "non-erodible" scale relations that appear to be viable for sand (*Ho et al.,* 2011).

Despite arguments to the contrary for other materials (e.g. *Sterk et al*., 1998), saltating snow models relate mass flux to estimated airborne surface shear stress. These estimates are often based on a momentum deficit derived from the total number of particles in transport, neglecting the vertical heterogeneity of particle concentration within the snow saltation layer (*Doorschot and Lehning*, 2002). As all panels in Fig. 6 and 7 show, uniform descriptions of surface shear stress calculations based solely on concentration and flux measurements above 10 mm overlook the immense wind momentum transferred into the creep layer (i.e. *Zhang et al.,* 2007, *Creyssels et al.,* 2009; *Ho et al.,* 2011, 2012, 2014). Disregarding this flux prevents calculation of an accurate momentum balance. Accounting for variability in saltation trajectories would also allow for a dense surface flow to be represented that can feed upper regions (e.g. *Nemoto and Nishimura*, 2004) and create a self-consistent momentum balance. *Andreotti* (2004) wrote a further discussion of self-consistency errors of wind feedback in single trajectory saltation models.

The wide variety of snow saltation initiation mechanisms observed in this experiment is in contrast to classic initiation models that assume that a temporally-constant fraction of saltating grains begin motion through either aerodynamic entrainment or splash (e.g. *Pomeroy and Gray*, 1990). As seen in Fig 9, in intermittent conditions this variability is magnified, as splash regimes themselves are intermittent, depending on sufficient wind speed for adequate particle acceleration upon ejection from the snow surface.

5 Conclusion

This is the first investigation to measure outdoor snow particle flux and velocity immediately above the snow surface. It provides an opportunity to test certain observations of saltating particle flux trajectories measured in wind tunnels. Though observations were restricted to moderate wind speeds and

Nik Aksamit 8/31/2016 2:41 PM
Deleted: are

Nik Aksamit 8/31/2016 2:41 PM
Deleted: here, highly

Nik Aksamit 8/31/2016 2:41 PM
Deleted: , preventing

Nik Aksamit 8/31/2016 2:41 PM
Deleted: bed descriptions

Nik Aksamit 8/31/2016 2:41 PM
Deleted: In equilibrium conditions, velocity and flux distributions found in sand studies confirm that the majority of saltation consists of particles tumbling over the surface, and that the properties of flow in the region below twice the Bagnold focus height govern the mean properties of saltating particles (*Creyssels et al*., 2009; *Ho et al.,* 2011, 2014). This region of particle transport is thus crucial for modeling features of the saltation cloud. Interestingly, sand particle motion in this region was found to be insensitive to increases in mean wind velocity. Presumably, as concentration increases, slip-velocities, u_0, return to mean values over time. It should be noted that while saturated equilibrium conditions were not found during any of the blowing snow recordings, and near-surface particle velocities reflected instantaneous wind speed fluctuations, u_0 values from snow were comparable to sand values and were insensitive to changes in mean wind speed. This resiliency may help explain some of the robustness of time-averaged uniform trajectory blowing snow models, but requires further investigation.

Nik Aksamit 8/31/2016 2:41 PM
Deleted: 3

Nik Aksamit 8/31/2016 2:41 PM
Deleted: (

Nik Aksamit 8/31/2016 2:41 PM
Deleted:)).

Nik Aksamit 8/31/2016 2:41 PM
Deleted: 4

Nik Aksamit 8/31/2016 2:41 PM
Moved down [8]: It could be very useful to compare modeled entrainment and splash ratios with PTV datasets, however longer recording times over a larger variety of snow types would be necessary to obtain statistically significant comparisons. Specifically, whether long time average stati ... [21]

Nik Aksamit 8/31/2016 2:41 PM
Deleted: The first environmental PTV computations for blowing snow have

Nik Aksamit 8/31/2016 2:41 PM
Moved (insertion) [5]

Nik Aksamit 8/31/2016 2:41 PM
Moved (insertion) [6]

intermittent transport, they show the importance of creep to blowing snow transport initiation and transition to full saltation. Being able to relate high frequency turbulent wind speed to snow transport (e.g. *Guala et al.*, 2008) is critical in the alpine environment (*Naaim-Bouvet et al.*, 2011) and this study makes a contribution to understanding these dynamics.

PTV has proven to be a viable avenue for exploring complex wind-snow interactions at millisecond timescales in natural, non-steady state, high Reynolds number wind conditions. These results support the need for further conceptual advancement of models of snow saltation, initiation and rebound, including multiple types of motion and the interaction of turbulent sweeps on particle erosion and entrainment. Over short timescales, snow particle behaviour is influenced by complex wind speed dependent initiation and rebound dynamics, including a variable dense surface flow that is beyond the scope of scalar aerodynamic entrainment and splash parameterizations. The wind-to-snow and snow-to-snow momentum transfer in the first few mm above the surface is critical for both driving mechanisms of transport initiation as well as providing lower boundary conditions for two-phase atmospheric flows. The combination of all results support a wide spectrum of particle motion exists in all recordings with surface and upper level transport intrinsically linked through momentum and mass balances. The roles of both surface and upper level transport depend on wind strength and snowpack properties. Sand saltation velocity distribution models do not comprehensively describe transport of complex snow crystal structures such as the previously undescribed tumblon motions or snow particle shattering and sintering. Low-energy near-surface particles contribute considerably to saltation through large particle number flux and by both bouncing into upper saltation regions and by breaking snow bed matrix bonds, making particles freely available for splash and entrainment with reduced wind drag requirements.

The ability of the snowpack surface to absorb wind and particle momentum in the dense surface region of saltation appears variable and substantial. The near-surface layer was observed to be the region of peak snow particle concentration. In the wind conditions investigated, this high particle concentration compensated for the reduced particle speeds near the surface, and sustained a layer of peak particle and likely mass flux. The creep layer has far more intricate dynamics and greater flux relevance than previously described, and is a dynamic zone of erosion and deposition during snow transport whilst

Nik Aksamit 8/31/2016 2:41 PM
Deleted: millimeters

Nik Aksamit 8/31/2016 2:41 PM
Deleted: A

Nik Aksamit 8/31/2016 2:41 PM
Deleted: was found

Nik Aksamit 8/31/2016 2:41 PM
Deleted: the majority of

Nik Aksamit 8/31/2016 2:41 PM
Deleted: Near

Nik Aksamit 8/31/2016 2:41 PM
Deleted: below 10 mm

feeding the saltation layer immediately above. Saltation dynamics are therefore dependent upon creep particle motions, which mediate exchange between the snow surface and blowing snow.

The role that creep plays in the surface momentum balance and mass flux appeared dependent on snow surface hardness. Wind-hardened surfaces shared several trends similar to that of rigid sand-beds, though not all wind-tunnel observations could be replicated. As creep in intrinsically linked to saltation through momentum redistribution and as a potential reservoir for saltating particles, creep dynamics changes over varying surface harnesses also result in changes in saltation dynamics, such as changes in velocity gradients, particle concentration, and rebound dynamics.

In the present study, the near-surface particle velocities reflected instantaneous wind speed fluctuations and never achieved equilibrium. As the snow is in constant readjustment to changes in wind velocity, and short time scale turbulence characteristics do not scale with long time averages, further characterizations of the time scale of relevance or relevant turbulence scaling relations in alpine terrain need to be performed before a steady-state equilibrium type saltation model (e.g. *Pomeroy and Gray*, 1990; *Doorschot and Lehning,* 2002) can be deemed appropriate for these situations. Furthermore, as contributions of shear stress from different quadrants are spatially and temporally variable and the mechanics of transport vary during gusts as seen in Section 3.3, the need to account for variable shear stress in high-resolution modeling (*Doorschot et al.*, 2004; *Groot Zwaaftink et al.*, 2014) is reinforced.

It could be very useful to compare modeled entrainment and splash ratios with PTV datasets, however longer recording times over a larger variety of snow types would be necessary to obtain statistically significant comparisons. Specifically, whether long time average statistics can account for periods of varying initiation during intermittent saltation, or only can apply in more nearly steady-state environments would be a useful finding for high temporal resolution applications (e.g. *Groot Zwaaftink et al.*, 2014).

Snow saltation velocities, heights, and particle concentrations responded on scales of < 1 s to turbulent wind speed fluctuations. Analysis of a turbulent sweep event has shown that snow transport is sensitive to different generators of RS. PTV shows potential to answer many open questions in blowing snow research through quantification of momentum redistribution in very near-surface particle motion. The use of high temporal-resolution outdoor PTV measurements may prove useful in future work for

Nik Aksamit 8/31/2016 2:41 PM
Moved (insertion) [7]

Nik Aksamit 8/31/2016 2:41 PM
Moved (insertion) [8]

Nik Aksamit 8/31/2016 2:41 PM
Deleted: Reynolds stress.

understanding the turbulent influences on intermittent blowing snow processes and allows comparison with and evaluation of wind tunnel PTV data.

6. ACKNOWLEDGEMENTS

The authors acknowledge funding from the Canadian Foundation for Innovation, the Natural Sciences and Engineering Research Council of Canada, the Changing Cold Regions Network, Canada Research Chairs, the Global Institute for Water Security and Alberta Agriculture and Forestry. The assistance of Nicolas Leroux and the Fortress Mountain Resort in logistics is gratefully noted. Data is available upon request directly from the authors, john.pomeroy@usask.ca.

References

Anderson, R. S. and Haff, P. K.: Simulation of eolian saltation, Science, 241(4867), 820–3, doi:10.1126/science.241.4867.820, 1988.

Anderson, R. S.: Eolian sediment transport as a stochastic process: The effects of a fluctuating wind on particle trajectories, J. Geol., 95(4), 497–512, doi:10.1086/629145, 1987.

Andreotti, B.: A two species model of aeolian sand transport, J. Fluid Mech., 510, 47–70, 2004.

Bagnold, R. A.: The physics of blown sand and desert dunes, 1st ed., Methuen & Co. Limited, London., 1941.

Bintanja, R.: Snowdrift suspension and atmospheric turbulence. Part I: Theoretical background and model description, Boundary-layer Meteorol., 95, 343–368, 2000.

Brown, T. and Pomeroy, J.: A blowing snow particle detector, Cold Reg. Sci. Technol., 16, 167–174, 1989.

Budd, W. F.: The drifting of non-uniform snow particles, in *Studies in Antarctic Meteorology, Antarctic Research Series 9*, edited by M. J. Rubin, pp. 59–70, American Geophysical Union, Washington D.C., 1966.

Nik Aksamit 8/31/2016 2:41 PM
Deleted: .,

Nik Aksamit 8/31/2016 2:41 PM
Deleted: Sediment Transport

Nik Aksamit 8/31/2016 2:41 PM
Deleted: Stochastic Process

Nik Aksamit 8/31/2016 2:41 PM
Deleted: Effects

Nik Aksamit 8/31/2016 2:41 PM
Deleted: Fluctuating Wind

Nik Aksamit 8/31/2016 2:41 PM
Deleted: Particle Trajectories

Nik Aksamit 8/31/2016 2:41 PM
Deleted: Physics

Nik Aksamit 8/31/2016 2:41 PM
Deleted: Blown Sand

Nik Aksamit 8/31/2016 2:41 PM
Deleted: Desert Dunes

Nik Aksamit 8/31/2016 2:41 PM
Formatted: Font:Times, English (US)

Budd, W. F., Dingle, W. R. J. and Radok, U.: The Byrd snow drift project: Outline and basic results, in Studies in Antarctic Meteorology, Antarctic Research Series 9 edited by M. J. Rubin, pp. 59–70, American Geophysical Union, Washington D.C., 1966.

Chapman, C. A., Walker, I. J., Hesp, P. A., Bauer, B. O. and Davidson-Arnott, R. G. D.: Turbulent Reynolds stress and quadrant event activity in wind flow over a coastal foredune, Geomorphology, 151-152, 1–12, doi:10.1016/j.geomorph.2011.11.015, 2012.

Creyssels, M., Dupont, P., El Moctar, a. O., Valance, A., Cantat, I., Jenkins, J. T., Pasini, J. M. and Rasmussen, K. R.: Saltating particles in a turbulent boundary layer: experiment and theory, J. Fluid Mech., 625, 47–74, doi:10.1017/S0022112008005491, 2009.

Dennis, D. J. C., and Nickels, T. B.: On the limitations of Taylor's hypothesis in constructing long structures in a turbulent boundary layer, J. Fluid Mech., *614*, 197, doi:10.1017/S0022112008003352, 2008.

Doorschot, J., Lehning, M. and Vrouwe, A.: Field measurements of snow-drift threshold and mass fluxes, and related model simulations, Boundary-Layer Meteorol., 347–368, 2004.

Doorschot, J. and Lehning, M.: Equilibrium saltation: mass fluxes, aerodynamic entrainment, and dependence on grain properties, Boundary-layer Meteorol., 104, 111–130, 2002.

Dyunin, A. K. and Kotlyakov, V.: Redistribution of snow in the mountains under the effect of heavy snow-storms, Cold Reg. Sci. Technol., 3, 287–294, 1980.

Ellis, J. T., Li, B., Farrell, E. J., and Sherman, D. J., Protocols for characterizing aeolian mass-flux profiles, *Aeolian Res.*, *1*(1-2), 19–26, doi:10.1016/j.aeolia.2009.02.001, 2009.

Fierz, C., Armstrong, R., Durand, Y., Etchevers, P., Greene, E., McClung, D. M., Nishimura, K., Satyawali, P. K. and Sokratov, S. A.: The international classification for seasonal snow on the ground, International Association of Cryospheric Sciences, 2009.

Foken, T.: *Micrometeorology*. Berlin: Springer, 2008. Print.

Foken, T. and Wichura, B.: Tools for quality assessment of surface-based flux measurements, Agric. For. Meteorol., 78, 83–105, doi:10.1016/0168-1923(95)02248-1, 1996.

Gauer, P.: Blowing and drifting snow in alpine terrain: A physically-based numerical model and related field measurements, Swiss Federal Institute of Technology Zurich, 1999.

Nik Aksamit 8/31/2016 2:41 PM
Deleted: a

Nik Aksamit 8/31/2016 2:41 PM
Deleted: a

Nik Aksamit 8/31/2016 2:41 PM
Deleted: J. J.

Nik Aksamit 8/31/2016 2:41 PM
Deleted: .,

Nik Aksamit 8/31/2016 2:41 PM
Deleted: Drifting Snow

Nik Aksamit 8/31/2016 2:41 PM
Deleted: Alpine Terrain

Nik Aksamit 8/31/2016 2:41 PM
Deleted: Physically-Based Numerical Model

Nik Aksamit 8/31/2016 2:41 PM
Deleted: Related Field Measurements

Nik Aksamit 8/31/2016 2:41 PM
Deleted: .,

George, W. K.: Is there a universal log law for turbulent wall-bounded flows?, Philos. Trans. A. Math. Phys. Eng. Sci., 365(1852), 789–806, doi:10.1098/rsta.2006.1941, 2007.

Gordon, M., Savelyev, S. and Taylor, P. A.: Measurements of blowing snow, part II: Mass and number density profiles and saltation height at Franklin Bay, NWT, Canada, Cold Reg. Sci. Technol., 55(1), 75–85, doi:10.1016/j.coldregions.2008.07.001, 2009.

Gordon, M. and Taylor, P. A.: Measurements of blowing snow, Part I: Particle shape, size distribution, velocity, and number flux at Churchill, Manitoba, Canada, Cold Reg. Sci. Technol., 55(1), 63–74, doi:10.1016/j.coldregions.2008.05.001, 2009.

Gromke, C., Horender, S., Walter, B. and Lehning, M.: Snow particle characteristics in the saltation layer, J. Glaciol., 60(221), 431–439, doi:10.3189/2014JoG13J079, 2014.

Groot Zwaaftink, C. D., Diebold, M., Horender, S., Overney, J., Lieberherr, G., Parlange, M. B. and Lehning, M.: Modelling small-scale drifting snow with a lagrangian stochastic model based on large-eddy simulations, Boundary-Layer Meteorol., doi:10.1007/s10546-014-9934-2, 2014.

Guala, M., Manes, C., Clifton, A. and Lehning, M.: On the saltation of fresh snow in a wind tunnel: Profile characterization and single particle statistics, J. Geophys. Res. Earth Surf., 113(3), 1–13, doi:10.1029/2007JF000975, 2008.

Helgason, W. and Pomeroy, J.: Uncertainties in estimating turbulent fluxes to melting snow in a mountain clearing, in Proc. 62nd Eastern Snow Conf., 129–142, 2005.

Ho, T. D., Dupont, P., Ould El Moctar, A. and Valance, A.: Particle velocity distribution in saltation transport, Phys. Rev. E - Stat. Nonlinear, Soft Matter Phys., 85(5), 1–5, doi:10.1103/PhysRevE.85.052301, 2012.

Ho, T. D., Valance, A., Dupont, P. and Ould El Moctar, A.: Aeolian sand transport: Length and height distributions of saltation trajectories, Aeolian Res., 12, 65–74, doi:10.1016/j.aeolia.2013.11.004, 2014.

Ho, T. D., Valance, A., Dupont, P. and Ould El Moctar, A.: Scaling laws in aeolian sand transport, Phys. Rev. Lett., 106(9), 4–7, doi:10.1103/PhysRevLett.106.094501, 2011.

Hutchins, N., Chauhan, K., Marusic, I., Monty, J., and Klewicki, J., Towards reconciling the large-scale structure of turbulent boundary layers in the atmosphere and laboratory, Boundary-Layer Meteorol., *145*(2), 273–306, doi:10.1007/s10546-012-9735-4, 2012.

Nik Aksamit 8/31/2016 2:41 PM
Deleted: a

Nik Aksamit 8/31/2016 2:41 PM
Deleted: a

Nik Aksamit 8/31/2016 2:41 PM
Deleted: Small-Scale Drifting Snow

Nik Aksamit 8/31/2016 2:41 PM
Deleted: Lagrangian Stochastic Model Based

Nik Aksamit 8/31/2016 2:41 PM
Deleted: Large-Eddy Simulations

Nik Aksamit 8/31/2016 2:41 PM
Deleted: a

Nik Aksamit 8/31/2016 2:41 PM
Deleted: , pp.

Nik Aksamit 8/31/2016 2:41 PM
Deleted: .,

Nik Aksamit 8/31/2016 2:41 PM
Formatted: Don't add space between paragraphs of the same style

Jackson, R. G.: Sedimentological and fluid-dynamic implications of the turbulent bursting phenomenon in geophysical flows, J. Fluid Mech., 77(03), 531, doi:10.1017/S0022112076002243, 1976.

Kinar, N. J. and Pomeroy, J. W.: Measurement of the physical properties of the snowpack, Rev. Geophys., 53, doi:10.1002/2015RG000481.Received, 2015.

Kobayashi, D.: Studies of snow transport in low-level drifting snow, Sapporo, Hokkaido, Japan., 1972.

Li, B. and McKenna Neuman, C.: Boundary-layer turbulence characteristics during aeolian saltation, Geophys. Res. Lett., 39(11), 1–6, doi:10.1029/2012GL052234, 2012.

Li, L. and Pomeroy, J. W.: Estimates of threshold wind speeds for snow transport using meteorological data, J. Appl. Meteorol., 36, 205–213, 1997.

Lü, X., Huang, N. and Tong, D.: Wind tunnel experiments on natural snow drift, Sci. China Technol. Sci., 55(4), 927–938, doi:10.1007/s11431-011-4731-3, 2012.

Maeno, N., Araoka, K., and Nishimura, K.: Physical aspects of the wind-snow interaction in blowing snow, *J. Fac. Sci. Hokkaido Univ.*, *6*(1), 127–141, 1980.

Mcelwaine, J. N., Maeno, N. and Sugiura, K.: The splash function for snow from wind-tunnel measurements, Ann. Glaciol., 38, 71–78, 2004.

Morris, S. C., Stolpa, S. R., Slaboch, P. E. and Klewicki, J. C.: Near-surface particle image velocimetry measurements in a transitionally rough-wall atmospheric boundary layer, J. Fluid Mech., 580, 319–338, doi:10.1017/S0022112007005435, 2007.

Naaim-Bouvet, F., Naaim, M., Bellot, H. and Nishimura, K.: Wind and drifting-snow gust factor in an Alpine context, Ann. Glaciol., 52(58), 223–230, doi:10.3189/172756411797252112, 2011.

Nemoto, M. and Nishimura, K.: Numerical simulation of snow saltation and suspension in a turbulent boundary layer, J. Geophys. Res., 109(D18), -, doi:10.1029/2004JD004657, 2004.

Nishimura, K. and Hunt, J. C. R.: Saltation and incipient suspension above a flat particle bed below a turbulent boundary layer, J. Fluid Mech., 417, 77–102, doi:10.1017/S0022112000001014, 2000.

Nishimura, K., Yokoyama, C., Ito, Y., Nemoto, M., Naaim-Bouvet, F., Bellot, H., Fujita, K., Yokoyama, C., Ito, Y., Nemoto, M., Naaim-bouvet, F., Bellot, H. and Fujita, K.: Snow particle speeds in drifting snow, J. Geophys. Res. Atmos., 119, 9901–9913, doi:10.1002/2014JD021686, 2014.

Nik Aksamit 8/31/2016 2:41 PM
Formatted: Don't add space between paragraphs of the same style

Nik Aksamit 8/31/2016 2:41 PM
Deleted: Snow Transport in Low-Level Drifting Snow

Nik Aksamit 8/31/2016 2:41 PM
Deleted: Threshold Wind Speeds

Nik Aksamit 8/31/2016 2:41 PM
Deleted: Snow Transport Using Meteorological Data

Nik Aksamit 8/31/2016 2:41 PM
Deleted: Splash Function

Nik Aksamit 8/31/2016 2:41 PM
Deleted: Snow From Wind-Tunnel Measurements

Nik Aksamit 8/31/2016 2:41 PM
Deleted: bouvet

Otsu, N.: A threshold selection method from gray-level histograms, IEEE Trans. Syst. Man. Cybern., SMC-9(1), 62–66, 1979.

Owen, P. R.: Saltation of uniform grains in air, J. Fluid Mech., 20(02), 225, doi:10.1017/S0022112064001173, 1964.

Paterna, E., Crivelli, P. and Lehning, M.: Decoupling of mass flux and turbulent wind fluctuations in drifting snow, *Geophys. Res. Lett.*, 1–7, doi:10.1002/2016GL068171, 2016.

Pomeroy, J. and Gray, D.: Saltation of snow, Water Resour. Res., 26(7), 1583–1594, 1990.

Pomeroy, J. W. and Male, D. H.: Steady-state suspension of snow, J. Hydrol., 136(1-4), 275–301, doi:10.1016/0022-1694(92)90015-N, 1992.

Pomeroy, J. W. and Gray, D. M.: *Snowcover: Accumulation, relocation, and management*, Saskatoon, SK., 1995. Print.

Pomeroy, J. and Li, L.: Prairie and Arctic areal snow cover mass balance using a blowing snow model, J. Geophys. Res., 105(D21), 26619–26634, 2000.

Pomeroy, J., Fang, X. and Ellis, C.: Sensitivity of snowmelt hydrology in Marmot Creek, Alberta, to forest cover disturbance, Hydrol. Process., 26(12), 1891–1904, doi:10.1002/hyp.9248, 2012.

Rosi, G. A., Sherry, M., Kinzel, M. and Rival, D. E.: Characterizing the lower log region of the atmospheric surface layer via large-scale particle tracking velocimetry, Exp. Fluids, 55(5), 10, doi:10.1007/s00348-014-1736-2, 2014.

Schmidt, R.A.: Threshold wind-speeds and elastic impact in snow transport, J. Glaciol., 26(94), 453–467, 1980.

Schmidt, R. A. Vertical profiles of wind speed, snow concentration, and humidity in blowing snow, *Boundary-Layer Meteorol.*, *23*, 223–246, doi:10.1016/j.soncn.2013.06.001, 1982.

Schmidt, R.A.: Measuring particle size and snowfall intensity in drifting snow, Cold Reg. Sci. Technol., 9, 121–129, 1984.

Schweizer, J., Jamieson, B. and Schneebeli, M.: Snow avalanche formation, Rev. Geophys., 41(4), doi:10.1029/2002RG000123, 2003.

Sørensen, M.: On the effect of time variability of the wind on rates of aeolian sand transport, Aarhus Geosci., 7, 73–77, 1997.

Deleted: Threshold Selection Method…hr [22]
Nik Aksamit 8/31/2016 2:41 PM
Formatted [23]
Nik Aksamit 8/31/2016 2:41 PM
Deleted: Pomeroy, J.
Nik Aksamit 8/31/2016 2:41 PM
Moved (insertion) [9] [24]
Nik Aksamit 8/31/2016 2:41 PM
Formatted [25]
Nik Aksamit 8/31/2016 2:41 PM
Formatted [26]
Nik Aksamit 8/31/2016 2:41 PM
Formatted [27]
Nik Aksamit 8/31/2016 2:41 PM
Formatted [28]
Nik Aksamit 8/31/2016 2:41 PM
Deleted: Acumulation, Relocation
Nik Aksamit 8/31/2016 2:41 PM
Formatted [29]
Nik Aksamit 8/31/2016 2:41 PM
Deleted: Management
Nik Aksamit 8/31/2016 2:41 PM
Moved (insertion) [10] [30]
Nik Aksamit 8/31/2016 2:41 PM
Moved up [9]: Pomeroy, J. and Gray, D [31]
Nik Aksamit 8/31/2016 2:41 PM
Moved up [10]: and Li, L.: Prairie and A [34]
Nik Aksamit 8/31/2016 2:41 PM
Deleted: . …,
Nik Aksamit 8/31/2016 2:41 PM
Moved up [11]: 105(D21), 26619–26634, 2000.
Nik Aksamit 8/31/2016 2:41 PM
Deleted: a
Nik Aksamit 8/31/2016 2:41 PM
Formatted [32]
Nik Aksamit 8/31/2016 2:41 PM
Formatted [33]
Nik Aksamit 8/31/2016 2:41 PM
Moved (insertion) [12] [35]
Nik Aksamit 8/31/2016 2:41 PM
Moved (insertion) [13] [36]
Nik Aksamit 8/31/2016 2:41 PM
Formatted [37]
Nik Aksamit 8/31/2016 2:41 PM
Deleted:
Nik Aksamit 8/31/2016 2:41 PM
Formatted [38]
Nik Aksamit 8/31/2016 2:41 PM
Deleted: Particle Size…article size and Sn [39]
Nik Aksamit 8/31/2016 2:41 PM
Deleted: Schmidt, R. A.: Properties of blo [40]
Nik Aksamit 8/31/2016 2:41 PM
Nik Aksamit 8/31/2016 2:41 PM
Formatted [41]
Nik Aksamit 8/31/2016 2:41 PM
[42]
Nik Aksamit 8/31/2016 2:41 PM

Sterk, G., Jacobs, a. F. G. and Van Boxel, J. H.: The effect of turbulent flow structures on saltation sand transport in the atmospheric boundary layer, Earth Surf. Process. Landforms, 23(10), 877–887, doi:10.1002/(SICI)1096-9837(199810)23:10<877::AID-ESP905>3.0.CO;2-R, 1998.

Stull, R.: An introduction to boundary layer meteorology, Kluwer Academic Publisher, Dordrecht, The Netherlands, 1988.

Sugiura, K. and Maeno, N.: Wind-tunnel measurements of restitution coefficients and ejection number of snow particles in drifting snow: determination of splash functions, Boundary-Layer Meteorol., 95(1), 123–143, 2000.

Sugiura, K., Nishimura, K., Maeno, N. and Kimura, T.: Measurements of snow mass flux and transport rate at different particle diameters in drifting snow, Cold Reg. Sci. Technol., 27(2), 83–89, doi:10.1016/S0165-232X(98)00002-0, 1998.

Tabler, R. D.: Snow transport as a function of wind speed and height, in Proceedings, Cold Regions Sixth International Specialty Conference TCCP/ASCE, pp. 729–738, Cold Regions Engineering, West Lebanon, NH., 1991.

Takeuchi, M.: Vertical profile and horizontal increase of drift-snow transport, J. Glaciol., 26(94), 481–492, 1980.

Toloui, M., Riley, S., Hong, J., Howard, K., Chamorro, L. P., Guala, M. and Tucker, J.: Measurement of atmospheric boundary layer based on super-large-scale particle image velocimetry using natural snowfall, Exp. Fluids, 55(5), 14, doi:10.1007/s00348-014-1737-1, 2014.

Tominaga, Y., Okaze, T., Mochida, A., Sasaki, Y., Nemoto, M. and Sato, T.: PIV measurements of saltating snow particle velocity in a boundary layer developed in a wind tunnel, J. Vis., 16(2), 95–98, doi:10.1007/s12650-012-0156-8, 2012.

Ungar, J. E. and Haff, P. K.: Steady state saltation in air, Sedimentology, 34(2), 289–299, doi:10.1111/j.1365-3091.1987.tb00778.x, 1987.

van Boxel, J., Sterk, G. and Arens, S.: Sonic anemometers in aeolian sediment transport research, *Geomorphology*, *59*(1-4), 131–147, doi:10.1016/j.geomorph.2003.09.011, 2004.

Nik Aksamit 8/31/2016 2:41 PM
Deleted: Introduction

Nik Aksamit 8/31/2016 2:41 PM
Deleted: Boundary

Nik Aksamit 8/31/2016 2:41 PM
Deleted: Meteorology

Nik Aksamit 8/31/2016 2:41 PM
Deleted: .,

Nik Aksamit 8/31/2016 2:41 PM
Deleted: Transport

Nik Aksamit 8/31/2016 2:41 PM
Deleted: Function

Nik Aksamit 8/31/2016 2:41 PM
Deleted: Wind Seep

Nik Aksamit 8/31/2016 2:41 PM
Deleted: Height

Nik Aksamit 8/31/2016 2:41 PM
Deleted: Profile

Nik Aksamit 8/31/2016 2:41 PM
Deleted: Horizontal Increase

Nik Aksamit 8/31/2016 2:41 PM
Deleted: Drift-Snow Transport

Vickers, D. and Mahrt, L.: Quality control and flux sampling problems for tower and aircraft data, J. Atmos. Ocean. Technol., 14(3), 512–526, doi:10.1175/1520-0426(1997)014<0512:QCAFSP>2.0.CO;2, 1997.

Willetts, B. B., McEwan, J. and Rice, M. A.: Initiation of motion of quartz sand grains, Acta Mech., 1, 123–134, 1991.

Willmarth, W. W. and Lu, S. S.: Structure of the Reynolds stress near the wall, J. Fluid Mech., 55(1), 65–92, doi:10.1017/S002211207200165X, 1972.

Winstral, A., Marks, D. and Gurney, R.: Simulating wind-affected snow accumulations at catchment to basin scales, Adv. Water Resour., 55, 64–79, doi:10.1016/j.advwatres.2012.08.011, 2013.

Zhang, W., Wang, Y. and Lee, S. J.: Two-phase measurements of wind and saltating sand in an atmospheric boundary layer, Geomorphology, 88(1-2), 109–119, doi:10.1016/j.geomorph.2006.10.017, 2007.

Zhu, W., van Hout, R. and Katz, J.: PIV measurements in the atmospheric boundary layer within and above a mature corn canopy. Part II: Quadrant-hole analysis, J. Atmos. Sci., 64(8), 2825–2838, doi:10.1175/JAS3990.1, 2007.

Nik Aksamit 8/31/2016 2:41 PM
Deleted: Measurements

Nik Aksamit 8/31/2016 2:41 PM
Deleted: Atmospheric Boundary Layer

Nik Aksamit 8/31/2016 2:41 PM
Deleted: Mature Corn Canopy.

Nik Aksamit 8/31/2016 2:41 PM
Deleted: Hole Analysis

Nik Aksamit 8/31/2016 2:41 PM
Deleted:

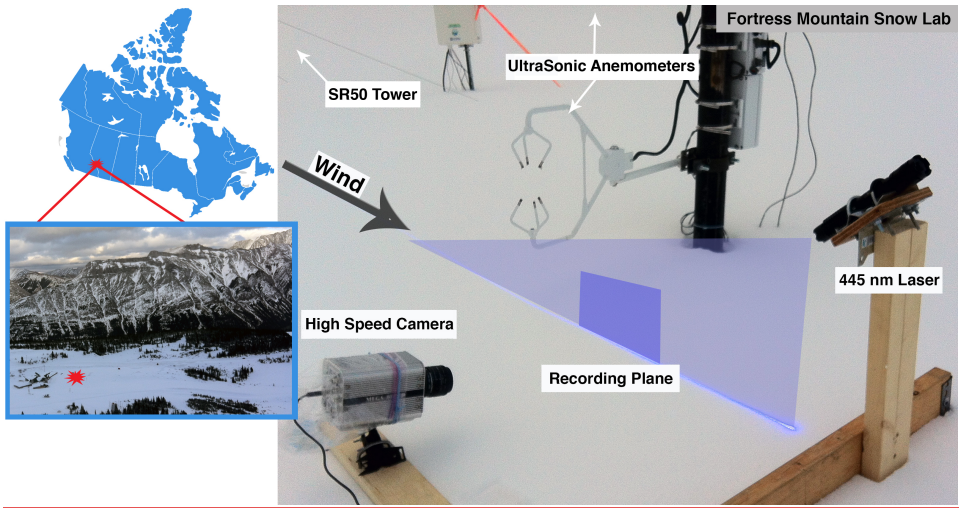

Figure 1: Blowing snow instrument setup and location of field site, Fortress Mountain Snow Laboratory, Alberta, Canada

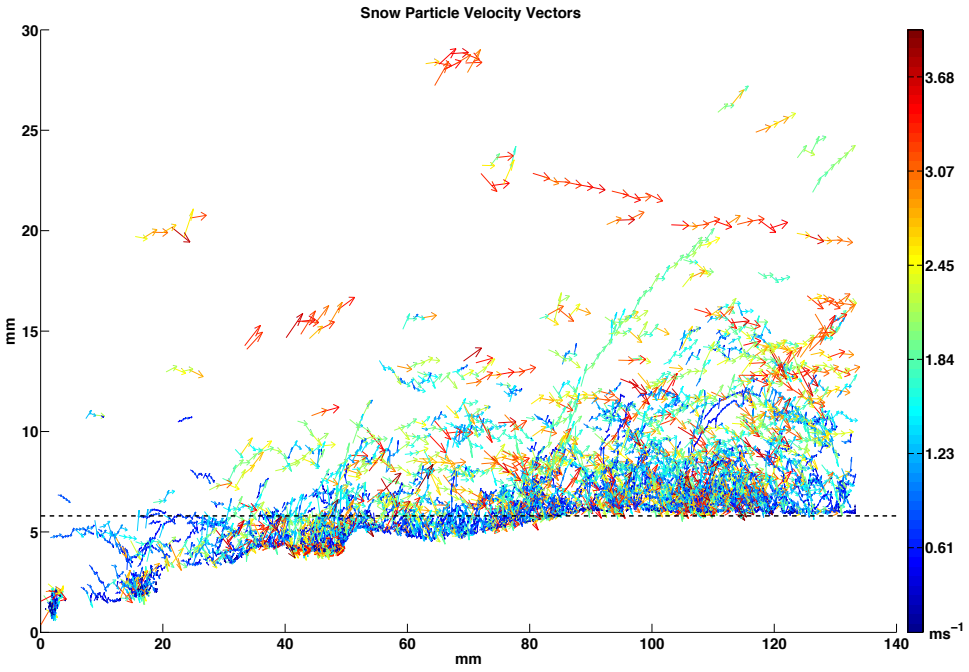

Figure 2: Sparse snow particle velocity vector field during one second of recording on 23 March, vector colors scaled according to total particle speed. The dashed line shows reference below which particles are influenced by microtopography.

Nik Aksamit 8/31/2016 2:41 PM

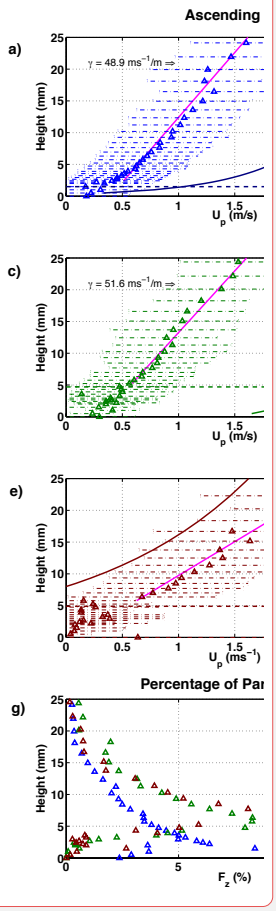

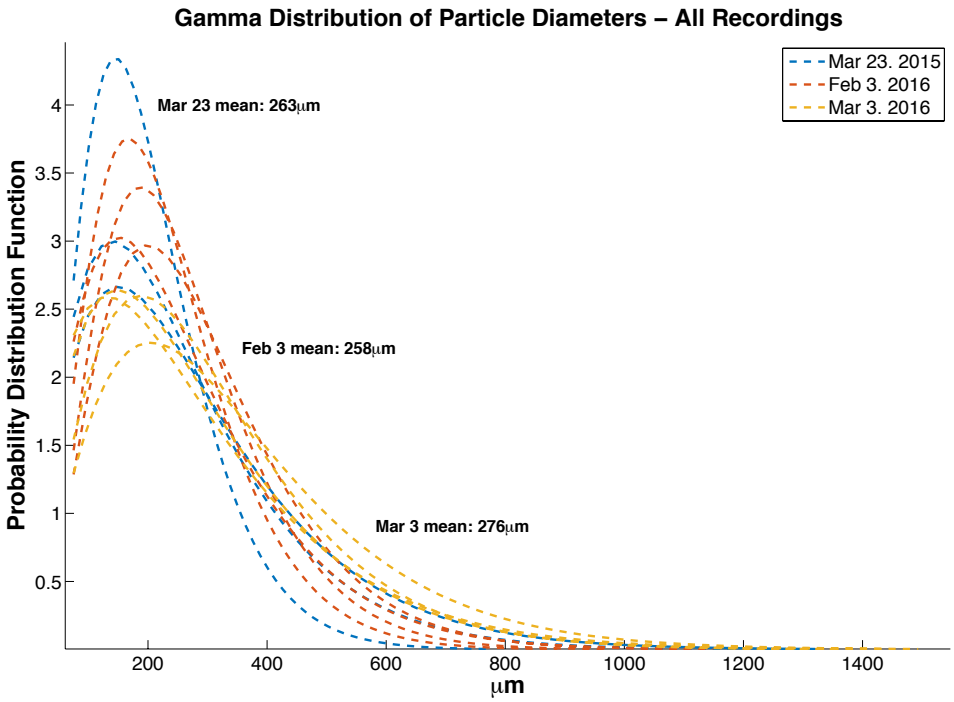

Figure 3: Two parameter Gamma distributions of particle diameters from each recording. Diameter measurements were obtained through black and white video binarization and equivalent diameter calculations of flood-fill identified connected components.

Nik Aksamit 8/31/2016 2:41 PM
Deleted: a-f): Ascending

Nik Aksamit 8/31/2016 2:41 PM
Deleted: descending mean

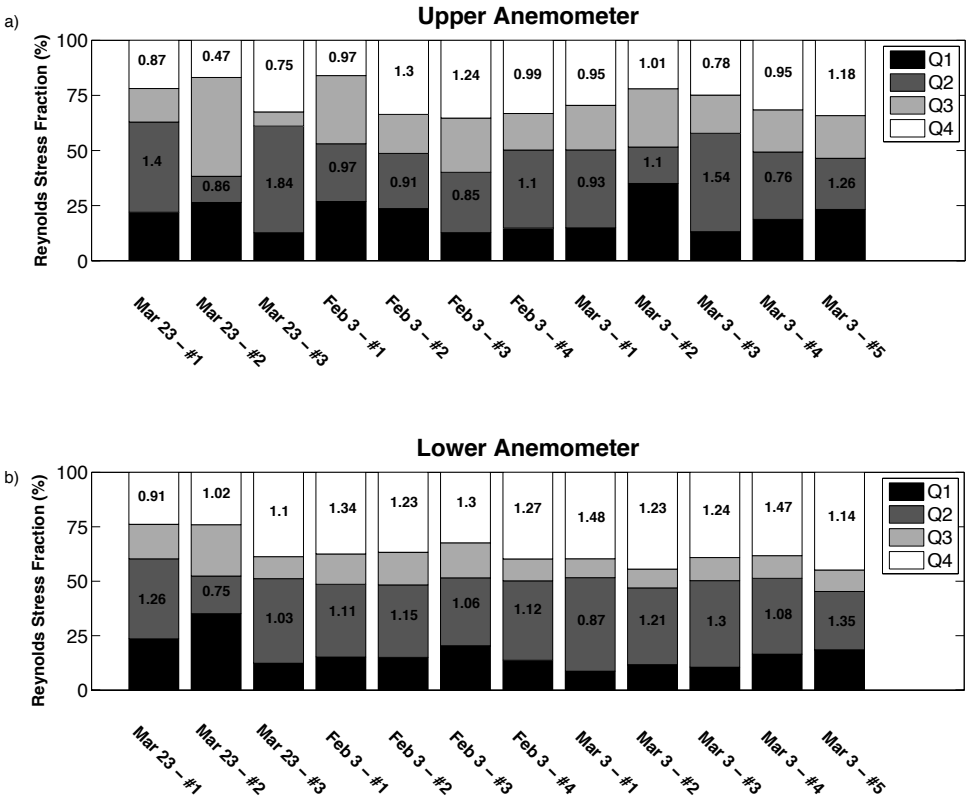

Figure 4: Percentage of Reynolds Stress distributed by Quadrants Analysis for 12 Blowing Snow Recordings with impact factor (% Stress/% Time) inset in Q2 and Q4 events. Note dominance of Q2 and Q4 generated stress. Mar 23 - #2 Low anemometer measurement contaminated.

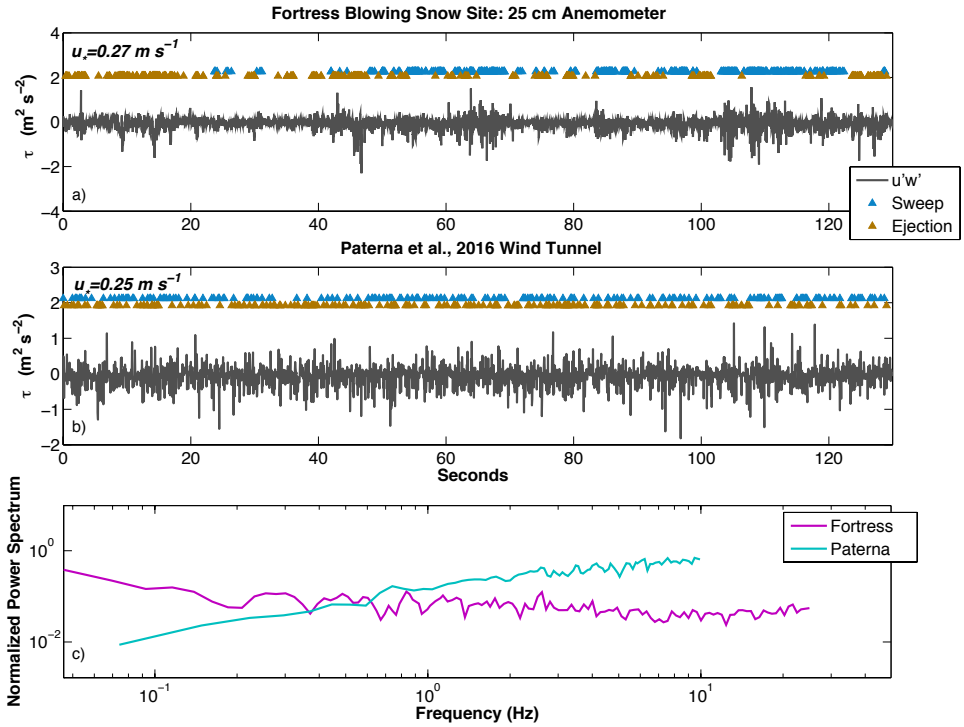

Figure 5: Plots a & b compare Reynolds Shear Stress signals from 3 February 2016 and Paterna et al. (2016) wind tunnel blowing snow studies. Triangles indicated Sweep and Ejection events larger than one standard deviation of Reynolds Stress. C) Normalized Power Spectral Density for streamwise velocity for the two time series.

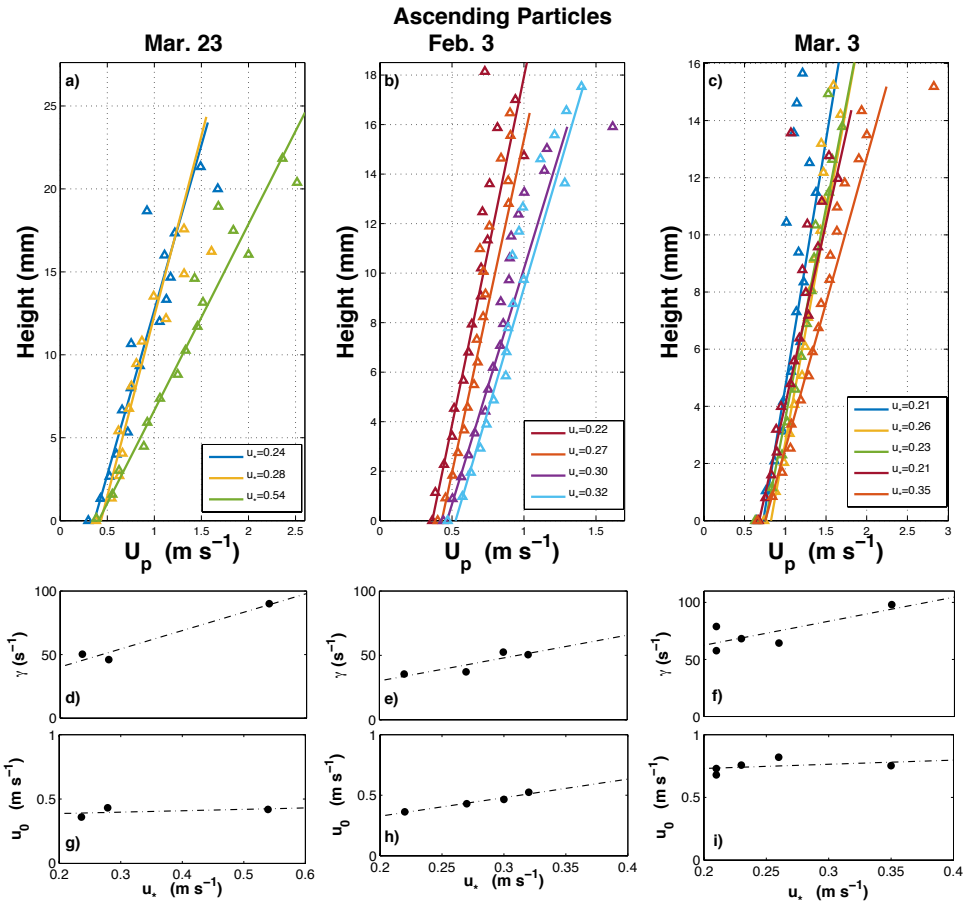

Figure 6: a-c) Average ascending snow particle horizontal velocities in lower saltation layer (triangles) with best fit linear profile for first 10 mm. u_* values are calculated from 200 cm, 25 cm, and 10 cm for Mar 23, Feb 3, and Mar 3, respectively. d-f) Friction velocity versus particle slip velocity (u_0) for each recording. g-i) Friction velocity versus particle velocity gradient (γ) for each recording.

Nik Aksamit 8/31/2016 2:41 PM
Deleted: velocity profiles (u_p), with one standard deviation error bars, log-law wind profiles for recording specific

Nik Aksamit 8/31/2016 2:41 PM
Deleted: (solid lines), and plots of constant $du_p/dz = \gamma$. 3g) Particle

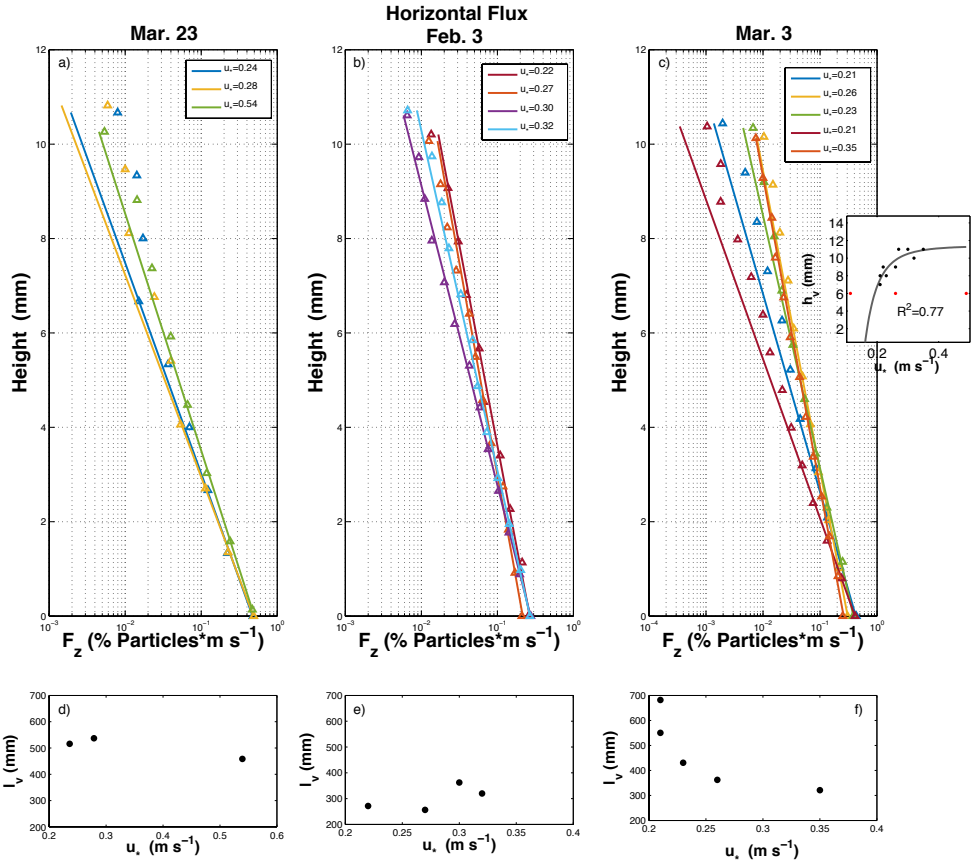

Figure 7: Plots a-c are mean horizontal flux measurements (F_z) and best fit exponential decay. Plots d-f are friction velocity versus decay length for each night. Friction velocity versus h_v (height below which 75% number flux occurred) for all nights with power law curve fitting is seen in the right inset. Values of h_v from 23 March 2015 are marked in red.

Nik Aksamit 8/31/2016 2:41 PM
Deleted: concentration profiles, 3h) Descending snow

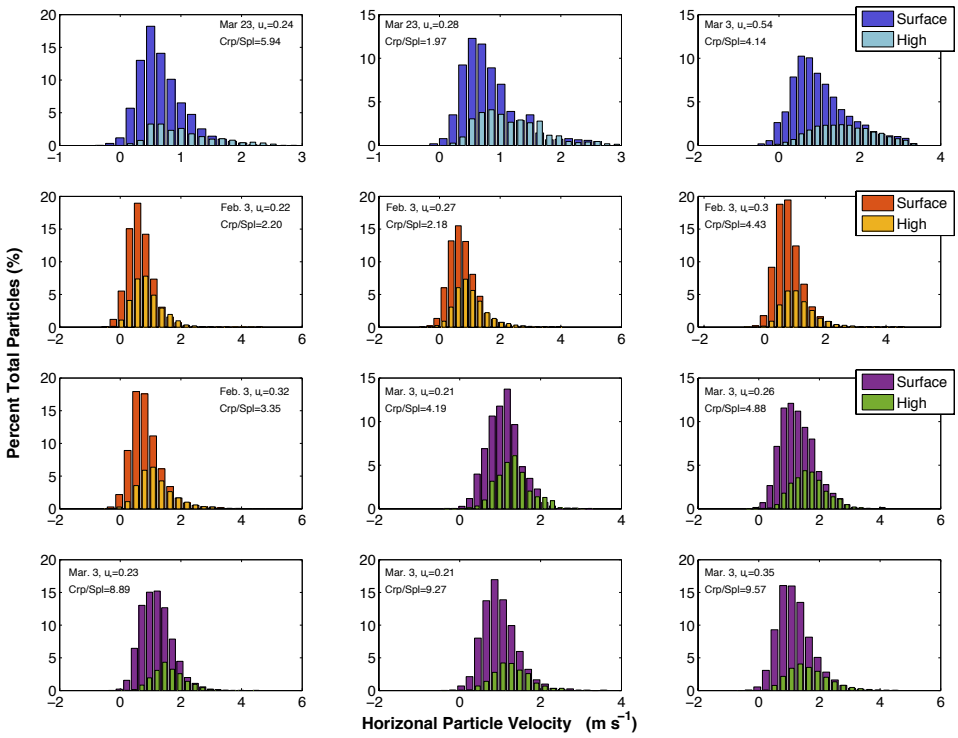

Figure 8: Horizontal particle velocity histograms for near-surface and upper region height bands for each recording over the three nights (each colored differently). Crp/Spl values indicate ratio of creep layer particle momentum to the contribution from saltating particle impacts.

Nik Aksamit 8/31/2016 2:41 PM
Deleted: two

Nik Aksamit 8/31/2016 2:41 PM
Deleted: the $u_* = 0.57\ ms^{-1}$ recording on March 23, 2015

Nik Aksamit 8/31/2016 2:41 PM
Deleted: <*sp*> ... [43]

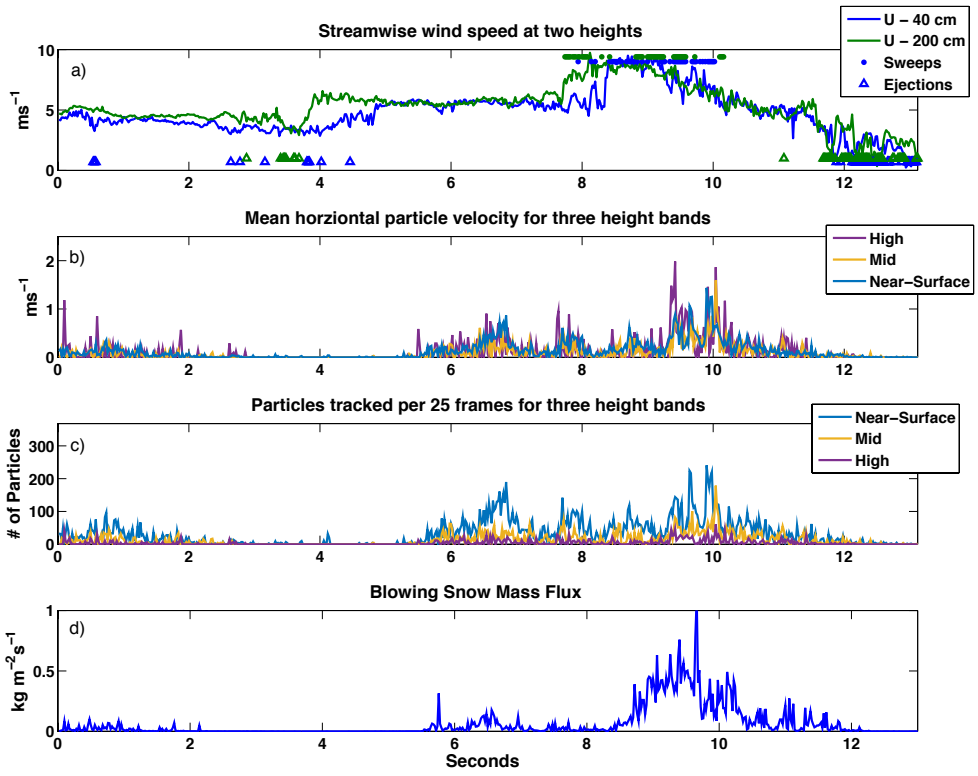

Figure 9: 23 March, recording #3 time series. a) 50 Hz streamwise wind speed at 40 and 200 cm above snow surface. b) 50 Hz Snow particle velocities obtained by binning particle vectors in three height bands (1<z<4 mm (Near-Surface), 4<z<8 mm (Mid), 8<z<30 mm (High)), then temporally averaged over 25 frames, c) Number of tracked particles in same height bands per 25 frames, d) Instantaneous blowing snow flux rates $Q_s\ (kg/m^2 s)$ (1250 Hz).

Nik Aksamit 8/31/2016 2:41 PM
Deleted: 4

Nik Aksamit 8/31/2016 2:41 PM
Formatted: English (UK)

Nik Aksamit 8/31/2016 2:41 PM
Deleted: 50Hz

Nik Aksamit 8/31/2016 2:41 PM
Formatted: English (UK)

Nik Aksamit 8/31/2016 2:41 PM
Formatted: English (UK)

Nik Aksamit 8/31/2016 2:41 PM
Deleted: averaging.

Nik Aksamit 8/31/2016 2:41 PM
Deleted: frame (1250 Hz),

Nik Aksamit 8/31/2016 2:41 PM
Formatted: English (UK)

Nik Aksamit 8/31/2016 2:41 PM
Formatted: English (UK)

Nik Aksamit 8/31/2016 2:41 PM
Deleted: *Otsu* (1979) binarization

Nik Aksamit 8/31/2016 2:41 PM
Formatted: English (UK)

Nik Aksamit 8/31/2016 2:41 PM
Deleted: particle pixel area per frame

Nik Aksamit 8/31/2016 2:41 PM
Formatted: English (UK)

Nik Aksamit 8/31/2016 2:41 PM
Deleted: Page Break
... [44]

Date	Snow surface conditions and weather	Density of loose surface grains	2 m Air/Snow Surface Temp	Surface Hardness (HHI)	Blowing Snow Grain Size (μm)
Mar. 23	5 cm graupel over old snow with light flurries	~350* (kg m^{-3})	-1C/(-)*	Fist over Melt-Freeze Crust (1 - 4)	263 (Max: 1200)
Feb. 3	Fine decomposing grains on windslab/sastrugi. No precip.	228 (kg m^{-3})	-10C/-10C	1 Finger-Pencil (3 - 4)	258 (Max: 850)
Mar. 3	Fresh snow. No precip.	156 (kg m^{-3})	-2C/-5C	Fist (1)	276 (Max: 2500)

Table 1: Descriptions of the snowpack for each night of recording including a description of the condition of the snow surface and concurrent precipitation, bulk density of the top 5 cm of grains, mean air temperature at the upper anemometer, snow surface temperature, hand surface hardness and HHI values following *Fierz et al.* (2009), as well as snow grain size as determined from the blowing snow video. *Density and Snow Surface temperature not available on March 23 with density estimated from *Pruppacher and Klett* (1997).

Nik Aksamit 8/31/2016 2:41 PM
Formatted: Font:9 pt

Nik Aksamit 8/31/2016 2:41 PM
Formatted: Font:Not Bold

Recording	Duration/Frames	$\bar{u}$ m s^{-1}	u_* m s^{-1}	z_0 mm	I %	S (non-dim)	Q_s kg m^{-2} s^{-1}
23/3/15 #1	7.3 s/9147						0.0146
200 cm		1.2 (5.5)	0.61 (0.23)	910.1 (0.1)	1.10 (0.22)	0.169 (0.028)	
40 cm		1.1 (4.7)	0.46 (0.26)	126.9 (0.3)	1.13 (0.27)	0.096 (0.034)	
23/3/15 #2	11.4 s/14299						2.54e-4
200 cm		1.9 (4.3)	0.48 (0.22)	410.6 (0.8)	1.04 (0.24)	0.139 (0.039)	
40 cm		1.7 (4.2)	0.40 (0.08)	69.9 (1.3 e-4)	1.04 (0.16)	0.096 (0.007)	
23/3/15 #3	13.1 s/16404						0.0237
200 cm		1.4 (5.3)	0.28 (0.55)	312.2 (42.4)	0.80 (0.40)	0.037 (0.148)	
40 cm		1.3 (4.8)	0.24 (0.57)	116.5 (8.0)	0.79 (0.45)	0.027 (0.122)	
3/2/16 #1	27.8 s/ 43075						0.0179
155 cm		4.67 (5.78)	0.27 (0.26)	1.7 (0.3)	0.39 (0.22)	0.038 (0.036)	
25 cm		3.96 (4.9)	0.29(0.22)	1.6 (0.06)	0.41 (0.21)	0.044 (0.026)	
3/2/16 #2	28.0 s/ 57487						0.0375
155 cm		3.91 (5.35)	0.22 (0.23)	1.8 (0.4)	0.45 (0.23)	0.025 (0.027)	
25 cm		3.33 (4.54)	0.22 (0.27)	1.0 (0.2)	0.46 (0.25)	0.025 (0.037)	
3/2/16 #3	28.1 s/ 57528						0.0547
155 cm		4.3 (5.7)	0.34 (0.45)	12.2 (12.5)	0.44 (0.27)	0.054 (0.106)	
25 cm		3.67 (4.7)	0.27 (0.3)	1.7 (0.7)	0.44 (0.27)	0.034 (0.045)	
3/2/16 #4	28.0 s/ 57409						0.044
155 cm		3.1 (6.94)	0.31 (0.33)	35.4 (0.4)	0.83 (0.17)	0.056 (0.055)	
25 cm		2.6 (5.66)	0.31 (0.33)	14.7 (0.4)	0.84 (0.2)	0.056 (0.055)	
3/3/16 #1	27.9 s/ 43182						0.0046
140 cm		5.33 (4.58)	0.30 (0.16)	1.7 (0.03)	0.28 (0.16)	0.035 (0.013)	
10 cm		4.3 (3.75)	0.23(0.21)	0.2 (0.3)	0.29 (0.19)	0.021 (0.021)	
3/3/16 #2	27.9 s/ 43182						0.1474
140 cm		4.33 (5.47)	0.25 (0.42)	1.8 (10)	0.3 (0.23)	0.030 (0.084)	
10 cm		3.57 (4.33)	0.20 (0.26)	0.3 (0.1)	0.3 (0.23)	0.019 (0.033)	
3/3/16 #3	27.9 s/ 43182						0.1561
140 cm		4.7 (5.5)	0.27 (0.23)	2 (0.04)	0.26 (0.16)	0.035 (0.02)	
10 cm		3.85 (4.6)	0.22 (0.20)	0.4 (0.1)	0.27 (0.18)	0.023 (0.026)	
3/3/16 #4	28.1 s/ 57528						0.0542
140 cm		4.6 (5.54)	0.58 (0.24)	82 (0.2)	0.53 (0.17)	0.149 (0.028)	
10 cm		3.7 (4.35)	0.45 (0.21)	15 (0.9)	0.54 (0.2)	0.09 (0.021)	
3/3/16 #5	28.1 s/ 57528						0.3467
140 cm		4.3 (6.06)	0.50 (0.31)	63 (0.8)	0.61 (0.36)	0.131 (0.046)	
10 cm		3.5 (4.73)	0.42 (0.35)	14 (2)	0.63 (0.4)	0.092 (0.06)	

Table 2: Wind characteristics: mean wind speed $\bar{u}$, friction velocity u_*, aerodynamic roughness height z_0, turbulence intensity I, and Shields Parameter S for recordings on Mar. 23, 2015, Feb. 3 and Mar. 3, 2016. Average values from the 15 minutes surrounding each recording (and recording-only period in parentheses) are shown for the two measurement heights. Estimates of blowing snow flux Q_s in $kg\ m^{-2}\ s^{-1}$ are included for recording only periods.

Formatted ... [45]
Nik Aksamit 8/31/2016 2:41 PM
Formatted ... [46]
Nik Aksamit 8/31/2016 2:41 PM
Formatted ... [47]
Nik Aksamit 8/31/2016 2:41 PM
Formatted Table ... [48]
Nik Aksamit 8/31/2016 2:41 PM
Formatted ... [49]
Nik Aksamit 8/31/2016 2:41 PM
Formatted ... [50]
Nik Aksamit 8/31/2016 2:41 PM
Deleted: Turb. Int.
Nik Aksamit 8/31/2016 2:41 PM
Inserted Cells ... [58]
Nik Aksamit 8/31/2016 2:41 PM
Inserted Cells ... [56]
Nik Aksamit 8/31/2016 2:41 PM
Inserted Cells ... [57]
Nik Aksamit 8/31/2016 2:41 PM
Formatted ... [51]
Nik Aksamit 8/31/2016 2:41 PM
Formatted ... [52]
Nik Aksamit 8/31/2016 2:41 PM
Formatted ... [53]
Nik Aksamit 8/31/2016 2:41 PM
Formatted ... [54]
Nik Aksamit 8/31/2016 2:41 PM
Formatted ... [55]
Nik Aksamit 8/31/2016 2:41 PM
Formatted ... [59]
Nik Aksamit 8/31/2016 2:41 PM
Formatted ... [60]
Nik Aksamit 8/31/2016 2:41 PM
Formatted ... [61]
Nik Aksamit 8/31/2016 2:41 PM
Formatted ... [62]
Nik Aksamit 8/31/2016 2:41 PM
Formatted ... [63]
Nik Aksamit 8/31/2016 2:41 PM
Moved down [14]: 1.10 (0.22)
Nik Aksamit 8/31/2016 2:41 PM
Formatted ... [64]
Nik Aksamit 8/31/2016 2:41 PM
Moved (insertion) [14] ... [65]
Nik Aksamit 8/31/2016 2:41 PM
Deleted: 1.13 (0.27)
Nik Aksamit 8/31/2016 2:41 PM
Formatted ... [66]
Nik Aksamit 8/31/2016 2:41 PM
Formatted ... [67]
Nik Aksamit 8/31/2016 2:41 PM
Formatted ... [68]
Nik Aksamit 8/31/2016 2:41 PM
Formatted ... [70]
Nik Aksamit 8/31/2016 2:41 PM
Inserted Cells ... [72]
Nik Aksamit 8/31/2016 2:41 PM
Formatted ... [75]
Nik Aksamit 8/31/2016 2:41 PM
Moved (insertion) [15] ... [73]
Nik Aksamit 8/31/2016 2:41 PM
Nik Aksamit 8/31/2016 2:41 PM
Formatted ... [76]
Nik Aksamit 8/31/2016 2:41 PM
Formatted ... [77]
Nik Aksamit 8/31/2016 2:41 PM
Moved (insertion) [16] ... [74]
Nik Aksamit 8/31/2016 2:41 PM
Nik Aksamit 8/31/2016 2:41 PM
Formatted ... [69]
Nik Aksamit 8/31/2016 2:41 PM
Formatted ... [71]
Nik Aksamit 8/31/2016 2:41 PM
Formatted ... [78]
Nik Aksamit 8/31/2016 2:41 PM
Formatted ... [79]